WAGENINGEN
UNIVERSITY & RESEARCH

Ready, aim, degranulate!
Molecular triggers of Natural Killer cells.

MSc Thesis

Natalia Rzepka (1256610)

Supervisors: Dr. Daan Vorselen & Dr. Christine Jansen

Cell Biology and Immunology (CBI)

03.09.2023 – 04.03.2024

Abstract

Natural killer (NK) cells are lymphocytes of the innate immune system displaying cytotoxic functions against tumours and viral-infected cells. A key component facilitating their cytotoxic activity is the formation of an immune synapse (IS). Establishing an IS is a multi-step, highly regulated process dependent on the signalling from integrins, activating and inhibitory receptors. However, there is currently little knowledge on the role of individual receptors and integrins in facilitating successful IS formation and degranulation. In this study we use deformable acrylamide acrylic acid particles (DAAM-Ps) functionalized with receptor-specific antibodies to delineate the roles of LFA-1 integrin and NKp30 activating receptor in IS formation and cytotoxicity of NK cells. We optimize protein A DAAM-P antibody functionalization to systematically trigger individual NK cell receptors. These assays reveal that LFA-1 is necessary for initial adhesion to the target, but requires NKp30 co-stimulation for degranulation. Additionally, we show that NKp30 activation is not sufficient for establishing an IS but increases complex formation when combined with suboptimal LFA-1 co-stimulation. Finally, we establish a novel method for imaging the IS in suspension cells by suspending preformed cell/DAAM-P complexes in agarose gel. Together this study lays the foundation for future research on the complex interactions at the immune synapse.

Table of contents

1. Introduction

Natural killer (NK) cells are granular lymphocytes of the innate immune system displaying both cytotoxic and cytokine-producing effector functions (Trinchieri, 1989). They can recognize tumour and stressed cells as targets to subsequently limit the spread of tissue damage and lower the risk of developing cancer (Imai et al., 2000). NK cells also play a crucial role in controlling viral infections, such as HIV-1 (Orange, 2006; Zuo & Zhao, 2021). As current treatment for HIV-1 is incapable of completely eradicating the virus, new promising therapy strategies involving the use of NK cells are emerging as an alternative (Duan & Liu, 2022). Another application that is currently of high interest is using CAR-NK cells as an alternative for CAR-T cell cancer therapy, with some CAR-NK cell treatment strategies already in clinical trials (Xie et al., 2020). Additionally, it has been shown that NK cells can act as regulatory cells on other components of the immune system. NK cells have been reported to kill previously activated CD4+ T cells as well as immature dendritic cells resulting in an anti-inflammatory effect (Lu et al., 2007; Piccioli et al., 2002; Rabinovich et al., 2003). This further broadens the potential application of NK cells in immunotherapy for autoimmune disorders and graft-versus-host disease.

NK cells can be divided into $CD56^{dim}$ and $CD56^{bright}$ subsets, both with their distinct roles. $CD56^{bright}$ cells are mostly present in secondary lymphoid tissues and are very efficient cytokine producers, while $CD56^{dim}$ cells are most abundant in peripheral blood and demonstrate high cytotoxic activity (Freud et al., 2017). As the $CD56^{dim}$ subset is mostly responsible for cell-killing, it will be the focus of this study.

Cytotoxic activity of activated NK cells, similarly to cytotoxic T cells (CTLs), is mediated by the release of lytic granules containing granzymes and perforin (Prager & Watzl, 2019). When released into the extracellular space perforin undergoes pH and Ca^{2+} dependent polymerization, creating perforin pores, through which granzymes can enter the cytoplasm of target cell. After entering the cytoplasm, granzymes trigger either caspase-mediated or caspase-independent apoptosis, effectively killing the cell (Voskoboinik et al., 2006).

Inititation of the NK cell cytotoxic response depends on the balance between activating and inhibitory signals on the target, which interact with a multitude of surface receptors on the NK cell. Depending on this balance, NK cells can then kill the target cell and release cytokines (Lanier, 2005). Important activating receptors include natural killer group 2 member D (NKG2D), NKp46 and NKp30. NKp46 and NKp30 are commonly called natural cytotoxicity receptors (NCRs) (Becker et al., 2016). NKp30 has been shown to interact with multiple, structurally different ligands, out of which two most relevant ones are BAT3 and B7-H6 proteins, which are upregulated on tumour cells (Pinheiro et al., 2020). Indeed, B7-H6 has been associated with the potential of NK cells to kill tumour cells and is considered a promising target for cancer immunotherapy (Cao et al., 2015). NKp46, on the other hand, has been associated with anti-viral protection, recognizing hemagglutinin in influenza and hemagglutinin neuraminidase in parainfluenza viruses (Mandelboim et al., 2001). Although endogenous ligands for NKp46 are mostly unknown, recently Sen Santara et al. (2023) identified that it recognizes externalized calreticulin as a danger-associated molecular pattern on ER-stressed cells. The NKG2D receptor is expressed by virtually all NK cells and it recognizes stress-induced ligands on target cells, namely MICA, MICB and ULBP1-6. The expression of these ligands is typically upregulated on tumour and virus-infected cells due to DNA damage, oxidative stress and hyperproliferation (Schmiedel & Mandelboim, 2018; Siemaszko et al., 2021).

The cytotoxicity of NK cells, however, is not as simple as a single chemical reaction of a receptor binding to its ligand but is a multi-step, regulated process. Crucial to this process is the formation of an immune synapse (IS) allowing close apposition and targeted degranulation to the target cell (**Figure 1**). Forming of the IS can be described in 3 general steps: initiation, effector and termination (Orange, 2008). In the initiation stage, it is thought that NK cell establishes a connection to the target cell through firm adhesion via integrins. (Barber et al., 2004). LFA-1 is thought to be particularly important in establishing the initial contact with the target. Upon clustering of integrins and conformational changes in the receptor, LFA-1 increases the binding activity to its ligand ICAM-1 and allows for adhesion (Kim et al.,

2011; Kinashi, 2005). However, it has also been shown before that the binding affinity of LFA-1 in NK cells can be regulated by intracellular signalling from activating receptors, questioning whether adherence is initiated solely through integrin interactions (Urlaub et al., 2017). Upon attachment to target cell, activating and inhibitory receptors start interacting with their ligands and the balance between their corresponding signals determines whether the IS will progress. When the NK cell is activated, in the effector stage, filamentous actin (F-actin) reorganizes at the synapse to form an enriched actin ring (resembling a round lamellipodium), followed by recruitment and clustering of activating receptors at the IS (Carisey et al., 2018). Through intracellular signalling from activating receptors lytic granules are then polarized to IS by moving towards the microtubule-organizing centre (MTOC) and this process is dependent on successful reorganization and integrity of F-actin (Carisey et al., 2018; Orange et al., 2003). In the final stage, after degranulation, signalling from activating receptors and their clustering at the IS is downregulated, the NK cell detaches and can move on to the next target.

Interestingly, although integrins are described in literature as indispensable during IS formation, recently it has been shown that NK cells can establish an IS and successfully degranulate just by crosslinking of NKG2D, without engagement of LFA-1 (Niek Frijlink, 2023). This surprising result questions the significance and precise role of integrin interactions in NK cell cytotoxicity. Additionally, with many activating and inhibitory receptors having been identified, the unique contributions of each individual receptor and LFA-1 integrin IS formation and cytotoxic activity are still largely unknown. Understanding how these separate receptors affect NK cell activity could enable the design of novel bispecific antibodies that optimally trigger NK cell responses as immunotherapy.

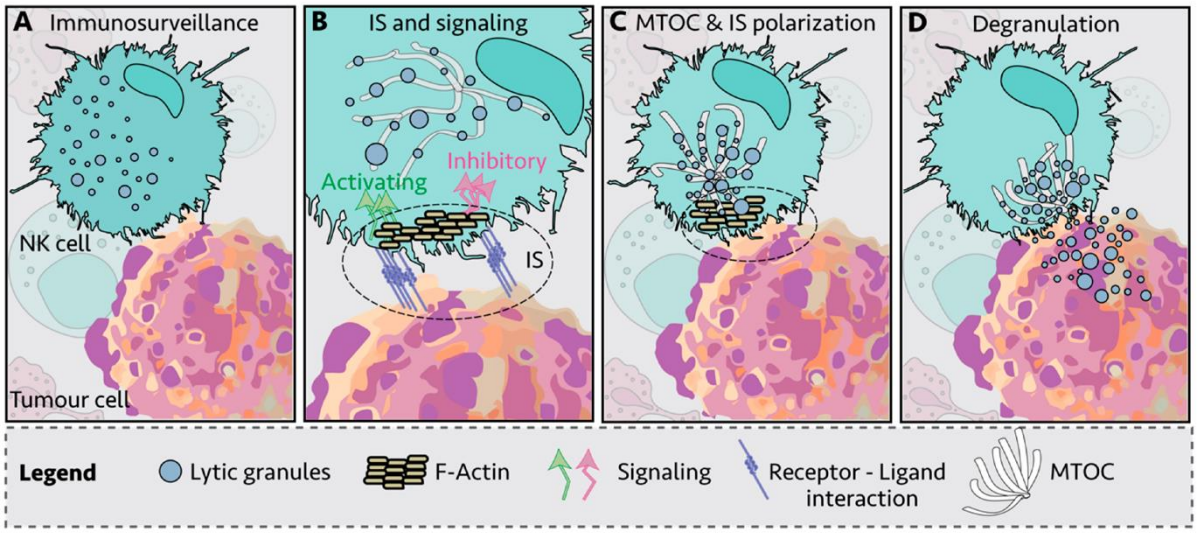

Figure 1. **Formation of the immune synapse (IS) between NK cell and a target cell.** If the cell is activated after adherence to target, activating receptors start clustering at the IS and filamentous actin (F-actin) rearranges to form an enriched actin ring. Lytic granules containing perforin and granzymes are then polarized to IS via microtubules and can be released to trigger target cell apoptosis Obtained from: (Meza Guzman et al., 2020).

In studying IS formation and cytotoxicity it is important to consider not only the chemical but also physical interactions between the NK cell and its target. Establishing an IS is a mechanosensitive process, requiring an optimal level of applied force by NK cells to maintain the cell-cell interaction. CTLs have been shown to have the ability to both sense and exert mechanical forces on their target and the same was hypothesized for NK cells (Huse, 2017; Vorselen et al., 2020). It has also been shown that both rigidity and size of targets significantly affects IS formation and degranulation in NK cells. However, most mechanistic studies focusing on IS formation use rigid and flat glass substrates (coated with ligands), because they allow easy visualization by microscopy. Using such high rigidity targets is suboptimal because it likely increases NK cell activation. Hence, here we will use specifically functionalized deformable acrylamide acrylic acid particles (DAAM-Ps) to identify the role of different activating receptors and the LFA-1 integrin in IS formation and NK cell cytotoxicity. DAAM-Ps are deformable microparticles of adjustable size and rigidity, that mimic mechanical properties of physiological NK cell target cells. Moreover, they allow for the calculation of mechanical forces and for

high resolution imaging due to their low optical distortion (Vorselen et al., 2020). However, DAAM particles have, so far, mostly been used to study phagocytosis, and significant functionalization and visualization challenges remain to study IS formation by (suspended) NK cells.

In this study, we develop and optimize a functionalization strategy of DAAM-Ps to activate NK cell cytotoxic IS formation one receptor at a time. We also describe a novel imaging method that allows for the visualization of IS formation on DAAM-Ps by NK cells without a disturbance to their physical structure. With these optimised assays, we show how a balance of LFA-1 integrins and activating receptors induces IS formation and cytotoxic activity in NK cells and discuss possible implications for future immunotherapy research.

2. Materials and methods

2.1. KHYG-1 cell culture

The immortalized NK cell line KHYG-1 (Leibniz Institute DSMZ, no. ACC 725) was cultured in medium RPMI 1640 (Gibco, Cat. No. 72400-021) with 10% FBS, 0,1% penicillin/streptomycin and 10 ng/ml IL-2 (Peprotech, Cat. No. 203-02) at 37 °C and 5% CO_2. To maintain IL-2 stability a stock of culture medium was prepared without IL-2 and the cytokine was added fresh to 50 ml batches of medium to the desired concentration of 10 ng/ml. After thawing, cells were cultured for a week in RPMI 1640 medium with 20% FBS, 0,1% penicillin/streptomycin and 10 ng/ml IL-2. Cells were passaged three times a week and maintained between 10^5 and $4{,}5x10^5$ cells/ml and a total volume of 15 ml in a T75 vent cap culture flask.

2.2. Staining surface receptors on KHYG-1 cells

Surface expression of receptors of interest was assessed prior to activation assays. To stain for LFA-1, NKp30 and NKp46 receptors corresponding specific primary antibodies were used, and MICA-Fc chimeric recombinant protein was used to stain NKG2D (**Table 1**.). Primary antibodies/recombinant proteins were detected using secondary antibodies labelled with a fluorophore (**Table 2.**). Two negative controls were included: control with cells only and one control without primary antibodies/recombinant proteins for each secondary antibody. All samples were done in triplicate.

Table 1. Primary antibodies and recombinant proteins used for staining surface receptors (N/A – not applicable).

Specificity	Host	Type	Clone	Company	CAT	Concentration
LFA-1	Rabbit	Monoclonal	1B4	Novus Biologicals	NBP3-09040	1; 5; 15 µg/ml
NKp30	Mouse	Monoclonal	210847	R&D Systems	MAB18491	0,1; 1; 10 µg/ml
NKp46	Rabbit	Polyclonal	N/A	Invitrogen	PA5-79720	0,1; 1; 10 µg/ml
MICA-Fc	Human	Recombinant protein	N/A	BioLegend	782706	0,1; 1; 10 µg/ml

Table 2. Secondary antibodies used for staining surface receptors.

Specificity	Host	Label	Company	CAT	Dilution
Human	Goat	AlexaFluor 488	Invitrogen	A55747	1:1000
Mouse	Goat	AlexaFluor 488	Invitrogen	A11001	1:1000
Rabbit	Goat	AlexaFluor 488	Invitrogen	A11008	1:1000

First, antibody or protein dilutions were prepared in cold FACS buffer (10 mg/ml BSA, 0,5 mM EDTA in PBS pH 7,4) at concentrations shown in Table 1 and 2 and kept on ice. KHYG-1 cells were collected from culture in a T75 flask, centrifuged at 500g for 5 min, resuspended in fresh culture medium and counted in a haemocytometer. After determining their concentration, cells were resuspended in FACS buffer at 500 000 cells/ml. To a 96-well round bottom plate 200µl of the new suspension (100 000 cells) was transferred per well and placed on ice. Plate was centrifuged for 2 min at 400g, supernatant removed by inverting the plate. Pellet was resuspended in primary antibody/recombinant protein solution (or FACS buffer for negative controls) and incubated on ice for 20 min. After incubation, plate was centrifuged again at 400g for 5 min, supernatant removed. Pellet was resuspended in corresponding secondary antibody solution (or FACS buffer for negative control) and incubated for 20 min on ice. Finally, the plate was centrifuged at 400g for 2 min, supernatant removed and pellet resuspended in FACS buffer. Samples were measured in a flow cytometer (CytoFLEX, Beckman Coulter) and analysed in FlowJo. A detailed staining protocol can be found in Appendix II.

2.3. DAAM-P functionalization with protein A and carboxyl-reactive dyes

Deformable acrylamide acrylic acid particles (DAAM-Ps) with the size of 14,7µm and rigidity of 5kPa were obtained from stock previously prepared by the lab of D. Vorselen (Vorselen et al., 2020).

DAAM-Ps were functionalized with protein A and carboxyl-reactive dyes. First, DAAM-Ps were diluted from 24% to 5% solids in activation buffer (100mM 2-(N-morpholino) ethane sulfonic acid (MES) buffer, pH 6 with 200mM NaCl) and maintained at 5% solids throughout the remaining steps. DAAM-Ps were washed twice in activation buffer by centrifuging for 1 min at 1000g and added to an activation mix containing 0,1% Tween20, 40 mg/ml N-(3-Dimethylaminopropyl)-N'-ethylcardbodimide hydrochloride (EDC) (Sigma-Aldrich, Cat. No. 25952-53-8) and 20 mg/ml N-Hydroxysuccimide (NHS) (Thermo Fisher Scientific, CAS-No. 6066-82-6). DAAM-Ps were incubated in activation mix for 15 min at room temperature (RT) while mixing. After incubation they were washed three times with 0,1x PBS (137 mM NaCl, 2,7 mM KCl, 8 mM Na_2HPO_4, 1,47 mM KH_2PO_4, pH 6) containing 0,2% Tween20 by centrifuging for 1 min at 1000g. DAAM-Ps were resuspended in 0,1x PBS pH 6 at half of the original volume and added to the same volume of 2x PBS pH 8,5. DAAM-Ps were mixed by pipetting up and down twice and transferred to a tube with protein A (SinoBiological, Cat. No. 10600-P07E) at a final protein concentration of 10 mg/ml. DAAM-Ps were incubated with the protein for 1h at RT while mixing. After incubation DAAM-Ps were directly transferred to a tube with carboxyl-reactive dyes: Fluorescein (FITC-) cadaverine (Thermofisher, Cat. No. 2415890) or Tetramethylrhodamine (TMR) cadaverine (Invitrogen, Cat. No. A1318) to a final dye concentration of 0,2 mM and incubated for 30 min at RT while mixing. After 30 min 0,5x current volume of blocking mix (100 mM tris(hydroxymethyl)aminomethane (Tris) pH 9, 100mM ethanolamine) was added and incubated for another 30 min at RT while mixing. Lastly, DAAM-Ps were washed three time with PBS pH 7,4 including 0,1% Tween20 by spinning 1 min at 1000g and resuspended in the original volume with the same PBS. Functionalized DAAM-P were stored at 4°C with 5mM sodium azide. A detailed protocol for DAAM-P functionalization can be found in Appendix II.

2.4. Coupling protein A DAAM-Ps with antibodies

DAAM-Ps functionalized with protein A and fluorescent dyes were further coupled with antibodies. Their overview and concentrations used are shown in **Table 3**. First, antibody/protein solutions were made in PBS of pH 7,4, 8, 8,5 or 9 at varying concentrations. Previously functionalized DAAM-Ps were centrifuged at 1000g for 1 min, resuspended in antibody/protein solutions and incubated for 1h at room temperature while shaking. After incubation DAAM-Ps were washed twice in PBS buffer (pH 7,4, 8, 8,5 or 9) with 0,1% Tween20 by centrifuging 1 min at 1000g. DAAM-Ps were resuspended in the same PBS and stored at 4°C (5mM sodium azide was added when stored for >1 day). When combining multiple antibodies on the same DAAM-Ps, they were incubated with the particles separately, including the washing steps in between. A detailed protocol can be found in Appendix II.

Table 3. Antibodies used for functionalizing protein A DAAM-Ps. (N/A – not applicable)

Specificity	Host	Type	Label	Clone	Company	CAT	Concentrations
Bovine	Rabbit	Polyclonal	FITC	N/A	Invitrogen	A24441	0,25; 0,8; 2,5; 8; 25µg/ml
LFA-1	Rabbit	Monoclonal	N/A	1B4	Novus Biologicals	NBP3-09040	0,25; 0,8; 2,5; 8; 25µg/ml
NKp30	Mouse	Monoclonal	N/A	210847	R&D Systems	MAB18491	0,25; 0,8; 2,5; 8; 25µg/ml

2.5. NK cell/DAAM-P complex formation assay

For the complex formation assays DAAM-Ps functionalized with a fluorophore, protein A and coupled with antibodies (see paragraph 2.4.) were used. First, KHYG-1 cells were collected from culture by centrifuging for 5 min at 500g and resuspended in fresh medium. Cell density was checked in a haemocytometer and cells were resuspended at 10^6 cells/ml in medium by centrifuging 5 min at 500g. New cell suspension was transferred to 14 ml round-bottom tubes to a final number of 500 000 cells per tube. DAAM-Ps were resuspended in medium by centrifuging for 1 min at 1000g and added to cells to reach approximately 10^6 DAAM-Ps per 500 000 cells. Samples were incubated at 37°C in a shaking incubator at 222 RPM. After 15 and 30 min from start of incubation 100 µl of all samples was taken out and pipetted through a 70µm cell strainer cap into 300µl cold FACS buffer (10 mg/ml BSA, 0,5 mM EDTA in PBS pH 7,4) and stored on ice. After 1h of incubation remaining volume of all samples was pipetted through a 70µm cell strainer cap into cold FACS buffer and stored on ice. Complex formation was measured on a flow cytometer (Beckman Coulter, Cytoflex-LX) and analysed in FlowJo. A detailed protocol can be found in Appendix II.

2.6. NK cell activation assay in PBMCs with degranulation marker CD107a

Peripheral blood mononuclear cells (PBMCs) were transferred from liquid nitrogen storage into a 37°C water bath. When only few ice crystals were visible, cells were transferred into a 15 ml tube and 13 ml of cold medium RPMI 1640 (Gibco, Cat. No. 72400-021) with 10% FBS, 0,1% penicillin/streptomycin was added drop wise. Cells were centrifuged at 280g for 5 min at 4°C. Supernatant was discarded, pellet was resuspended in 15 ml cold medium. Cells were centrifuged at 280g for 5 min at 4°C. Supernatant was discarded, pellet was resuspended in 6 ml cold medium. Cells were counted in a haemocytometer with Trypan Blue and resuspended at $2x10^6$ cells/ml. 250 µl cell suspension (500 000 cells) was transferred to each 14 ml round bottom tube. DAAM-Ps functionalized with FITC-cadaverine, protein A and coupled with anti-LFA-1 antibodies and anti-NKp30 antibodies (see paragraph 2.4) were resuspended in 250 µl medium and added to cells in a 2:1 ratio. 250 µl medium was added to unstimulated cells and to positive control. Anti-CD107a-eFluor 660 rat antibody (Invitrogen, clone 1D4B, Cat. No. 50-1071-82) was added to each sample to reach 2,5 µg/ml. BD GolgiStop (BD Biosciences, Cat. No. 512092KZ) was added to each sample at a 1:1000 dilution. Ionomycin (Merck, Cat. No. I0634-1MG) at 5 ng/ml and PMA (Merck, Cat. No. P8139-1MG) at 1 ng/ml were added to positive control samples. Samples were incubated at 37°C in a shaking incubator at 222 RPM. After 30 min first set of samples was pipetted through a 70 µm strainer cap into FACS tubes, placed on ice and washed with cold FACS buffer. Tubes were centrifuged at 280g for 3 min at 4°C, resuspended in 200 µl FACS buffer and stored at 4°C. After 4h second set of samples was pipetted through a 70 µm strainer cap into FACS tubes, placed on ice and washed with cold FACS buffer. Tubes from 30 min and 4h were centrifuged at 280g for 3 min at 4°C and pellet resuspended in a 1:25 dilution of mouse anti-human CD56-PE antibody (BioLegend, clone 5.1H11, Cat. No. 362524). Samples were incubated on ice, in the dark for 20 min. Samples were washed with cold FACS buffer, centrifuged for 5 min at 280g, 4°C. Supernatant was discarded, pellet resuspended in 200 µl FACS buffer. Before measuring 5 µl of 7-AAD marker (BD Bioscences, Cat. No. 5168981E) was added to every tube and mixed by pipetting. Samples were measured on a flow cytometer (Beckman Coulter, Cytoflex-LX). Compensation of overlapping signals was done using UltraComp eBeads Plus Compensation Beads (Invitrogen, Cat. No. 01333342), unstained cells and FITC-coupled DAAM-Ps. A detailed protocol can be found in Appendix II.

2.7. Imaging of immune complexes

To image immune synapse formation, first an activation assay was performed using DAAM-Ps functionalized with Tetramethylrhodamine (TMR) cadaverine (Invitrogen, Cat. No. A1318), protein A and coupled with antibodies. KHYG-1 cells were collected from culture by centrifuging for 5 min at 500g and resuspended in fresh medium. Cells were counted in a haemocytometer and resuspended at 10^6 cells/ml in medium by centrifuging 5 min at 500g. New cell suspension was transferred to 14 ml round-bottom tubes to a final number of 500 000 cells per tube. DAAM-Ps were resuspended in medium by centrifuging for 1 min at 1000g and added to cells at different time points to reach a 2:1 DAAM-P to cell ratio. Samples were incubated at 37°C in a shaking incubator at 222 RPM. After incubation samples were pipetted through a 70µm filter and then mixed 1:1 with 8% solution of paraformaldehyde (PFA) in PBS pH 7,4 and incubated for 10 min at RT. After this step different strategies for cell staining and immobilization were attempted. A detailed protocol can be found in Appendix II.

2.7.1. Staining in suspension with subsequent embedding in agarose

After incubation with PFA, samples were washed once with PBS pH 7,4 + 30 mg/ml BSA by centrifuging at 1000g for 3 min. Pellet was resuspended with 0,2% Triton X-100 (Merck, Cat. No. 9002-93-1) solution in PBS 7,4 + 30 mg/ml BSA and incubated for 10 min at RT. Samples were washed once with PBS pH 7,4 + 30 mg/ml BSA by centrifuging at 1000g for 3 min. Pellet was resuspended in 0,15 µM Phalloidin conjugated with AlexaFluor488 (Invitrogen, Cat. No. A12379) solution in PBS 7,4 + 30 mg/ml BSA and incubated for 30 min in the dark, at RT while shaking. Samples were washed once with PBS pH 7,4 + 30 mg/ml BSA by centrifuging at 1000g for 3 min and pellet was resuspended in 100µl PBS pH 7,4. Agarose (Eurogentec, Cat. No. EP-0010-05) in water solutions were prepared by microwaving in an Erlenmeyer flask until all the powder dissolved. Samples were mixed with liquid agarose at different concentrations:

- 100µl sample mixed with 100µl 1% agarose
- 100µl sample mixed with 900µl 0,5% agarose

Samples in agarose were transferred to empty wells of a 24 Well Glass Bottom Plate (Cellvis, Cat.No. P24-1.5H-N) and left to solidify at RT. Samples were stored in PBS pH 7,4 with 0,5mM sodium azide, at 4°C in the dark.

2.7.2. Staining after embedding in agarose

After incubation with PFA, samples were centrifuged at 500g for 3 min and resuspended in 100µl PBS pH 7,4. Agarose (Eurogentec, Cat. No. EP-0010-05) in water solutions were prepared by microwaving in an Erlenmeyer flask until all the powder dissolved and the samples were mixed with liquid agarose at different concentrations:

- 100µl sample mixed with 100µl 1% agarose
- 100µl sample mixed with 900µl 0,5% agarose

Samples in agarose were transferred to empty wells of a 24 Well Glass Bottom Plate (Cellvis, Cat.No. P24-1.5H-N) and left to solidify at RT. After the gel has solidified, a 0,2% Triton X-100 (Merck, Cat. No. 9002-93-1) solution in PBS pH 7,4 was added to wells and incubated at RT for 1h. After incubation wells were washed once with PBS pH 7,4 by inverting the plate and removing fluid from the gel. 0,15 µM Phalloidin conjugated with AlexaFluor488 (Invitrogen, Cat. No. A12379) solution in PBS 7,4 with 5mM sodium azide was added to wells and incubated overnight while shaking in the dark at RT. Next day, wells were washed once with PBS pH 7,4. Samples were stored in PBS pH 7,4 with 0,5mM sodium azide, at 4°C in the dark.

2.7.3. Confocal Microscope imaging

Nikon Ti2 microscope with a 40x lens, LED illumination source and EMCCD camera (Andor) was used to image preformed fluorescent NK cell/DAAM-P complexes. For each sample on a 24 Well Glass Bottom Plate five locations were chosen at random and images were analysed in ImageJ. Line profiles were created for ten different cells at multiple locations in every sample. Signal to noise (SNR) ratios were calculated for every cell based on **Equation 1**.

$$\mathrm{SNR} = \frac{\overline{\mathrm{S_C}} - \overline{\mathrm{S_B}}}{\mathrm{STD_B}}$$

Equation 1. Signal to noise (SNR) ratio equation. $\overline{S_c}$ – mean cell signal, $\overline{S_B}$ – mean background signal, $\mathrm{STD_B}$ – standard deviation of the background signal.

These ratios were then plotted for all tested conditions and the statistical significance of differences between them was assessed via one-way ANOVA test in GraphPad Prism.

3. Results

3.1. Optimisation of antibody binding to protein A on DAAM-Ps

In order to use DAAM-Ps for NK cell activation and IS visualisation we chose a functionalization approach using protein A, antibodies and a fluorophore-cadaverine conjugate. A simplified overview of this process can be seen in **Figure 2A**. This approach was chosen for its flexibility, adaptability to triggering different receptors and for the fact that it did not require any additional modifications of the IgGs themselves. Protein A and the cadaverine were covalently coupled to DAAM-Ps through amide bond formation. Receptor-specific antibodies were then used to target IgG-binding domains on protein A via their Fc region (Taylor et al., 2006). Due to this binding specificity the Fab region remained free and could bind to specific NK cell receptors and activate IS formation.

To optimise the conditions for antibody binding to protein A on DAAM-Ps, DAAM-Ps were first functionalized with protein A and TMR-cadaverine. Then, rabbit IgG conjugated with FITC was bound to the DAAM-Ps at concentrations ranging from 0,25 µg/ml to 25 µg/ml and PBS buffer of pH 7,4 and 8 were used. Samples were measured on a flow cytometer at 561 nm and 488 nm, background corrected and compensated for overlap between TMR and FITC. FITC fluorescence from IgG rose proportionally with antibody concentration, with 25 µg/ml IgG resulting in highest intensity at 488nm (**Figure 2B**). Additionally, FITC signal increased significantly where PBS pH 8 was used, in comparison to pH 7,4. To further optimize antibody binding, we used an IgG concentration of 25 µg/ml and tested higher pH PBS buffers, up to pH 9. The antibody (FITC) signal showed a notable increase with the rise in pH, with the highest intensity measured where PBS pH 9 was used (~15% higher than at pH 7.4) **(Figure 2C**). Based on these results, PBS pH 9 was chosen for antibody binding in all following assays.

Additionally, stability of protein A DAAM-Ps was tested by functionalization with the same rabbit IgG and flow cytometry analysis over time. No change in stability or functionalization efficiency was observed over the course of 7 weeks post functionalization, making it a safe storage time (**Figure S5**).

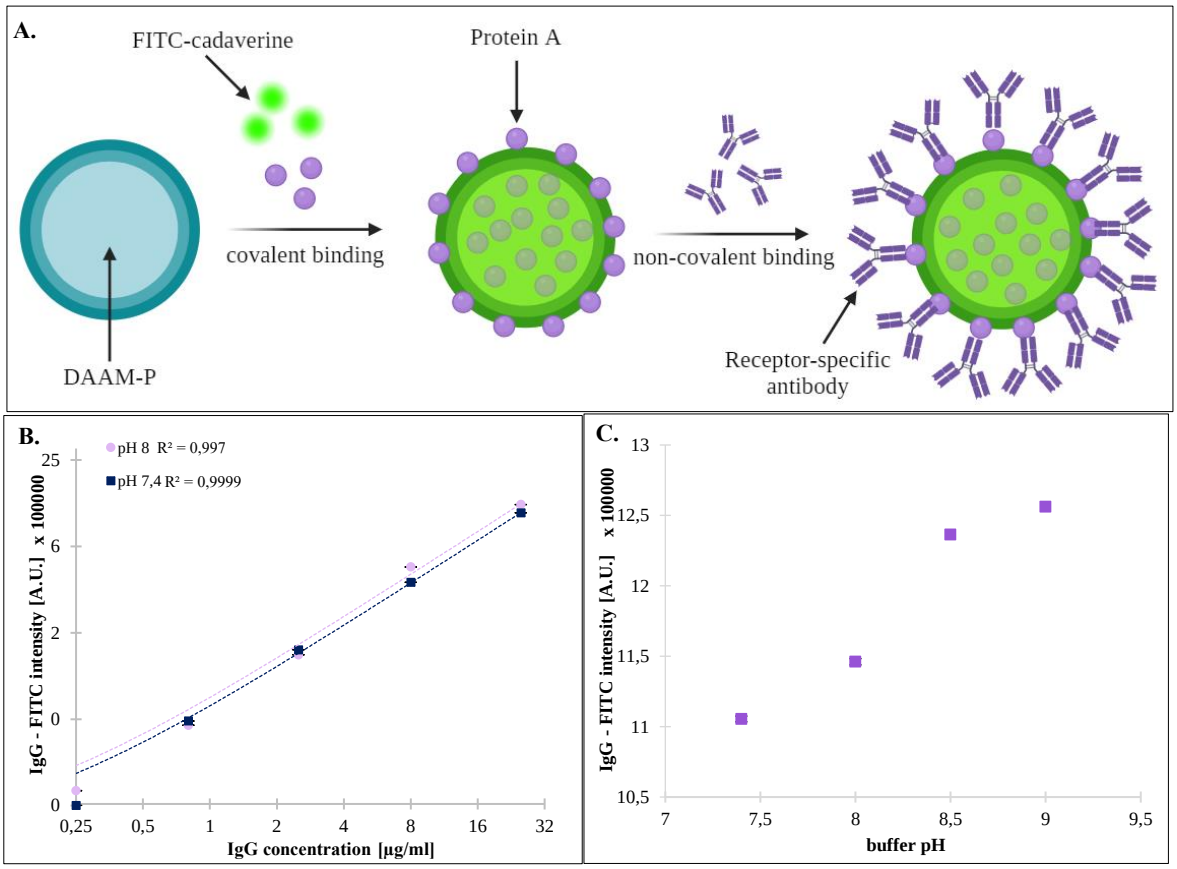

Figure 2. Optimisation of antibody binding to protein A. A. Simplified scheme of DAAM-P functionalization with protein A, fluorophore and antibodies. After activation with carboxyl-reactive chemical compounds: carbodiimide N-(3-Dimethylaminopropyl)-N'-ethylcardbodimide hydrochloride (EDC) and N-Hydroxysuccimide (NHS), amine groups from protein A and the cadaverine crosslink with carboxyl groups on DAAM-P creating covalent bonds. Antibodies can then bind non-covalently to protein A via their Fc domain, leaving the Fab region exposed (Created with BioRender). **B.** Binding efficiency of FITC-labelled rabbit IgG to DAAM-Ps in pH 7,4 or pH 8 at IgG concentrations between 0,25 and 25 µg/ml. Linear trend lines with corresponding R^2 values are included. **C.** Binding efficiency of FITC-labelled rabbit IgG to DAAM-Ps in different pH at an IgG concentration of 25 µg/ml. Error bars are present but are smaller than marker size and represent the standard error of the mean (SEM) of FITC signal within one sample. Coupling of antibodies to DAAM-Ps functionalized with protein A and TMR-cadaverine was performed in different pH PBS buffers. Fluorescence signal of FITC was measured at 488nm, background corrected and compensated for overlap with TMR.

3.2. Optimisation of staining assays in experiments with protein A DAAM-P

Using protein A DAAM-Ps creates a limitation in using additional cellular stains, as antibodies will non-specifically bind to protein A on DAAM-Ps via their Fc domain. However, antibodies differ in their binding efficiency to protein A depending on their subclass and species of origin (Hober et al., 2007). Here we explored the possibility of using antibodies from rats, which have a low binding efficiency to protein A in chromatography, in staining assays with DAAM-Ps. We compared this approach with using mouse IgGs, which are known to have very high binding affinity to protein A (New England Biolabs, 2024).

To optimise the staining method in protein A DAAM-P-based experiments we functionalized DAAM-Ps with FITC-cadaverine and protein A and stained them with antibodies of rat or mouse origin to test for differences in binding. Note that the species of origin and not the specificity of chosen antibodies was the main focus of this experiment. First, DAAM particles were stained with an NK cell marker, mouse anti-human CD56-PE for 4h. For comparison peripheral blood mononuclear cells (PBMCs) were incubated with the same marker and DAAM-Ps functionalized with 2,5 µg/ml anti-LFA-1 antibodies. Live lymphocytes were then gated based on their scattering properties and the 7-AAD live/dead marker (**Figure S3**). From all lymphocytes, cell/DAAM-P complexes were chosen based on their FITC signal. We then attempted to identify NK cells in complexes based on the CD56 marker. However, the antibody

of mouse origin bound to protein A on DAAM-Ps generating an overlapping signal for all lymphocytes in complexes, making the identification of cells expressing CD56 impossible (**Figure 3**, top).

To test if using antibodies from a different species could prevent such issues, DAAM-Ps were incubated with a degranulation marker, rat anti-CD107a-eFluor660 antibodies, for 4h. For comparison PBMCs were incubated with DAAM-Ps functionalized with 0,25 µg/ml anti-LFA-1 + 25 µg/ml anti-NKp30 antibodies, GolgiStop and the same degranulation marker. Live lymphocytes were then selected based on their scattering properties and the 7-AAD live/dead marker. From all lymphocytes, cell/DAAM-P complexes were chosen based on their FITC signal. CD107a staining was then compared between activated lymphocytes in cell/DAAM-P complexes and DAAM-Ps. In this case there was a clear difference in populations, with a distinguishable shift of activated lymphocytes in comparison to the signal from DAAM particles (**Figure 3**, bottom). Based on this, antibodies of rat origin were chosen for future staining assays in protein A DAAM-P-based experiments.

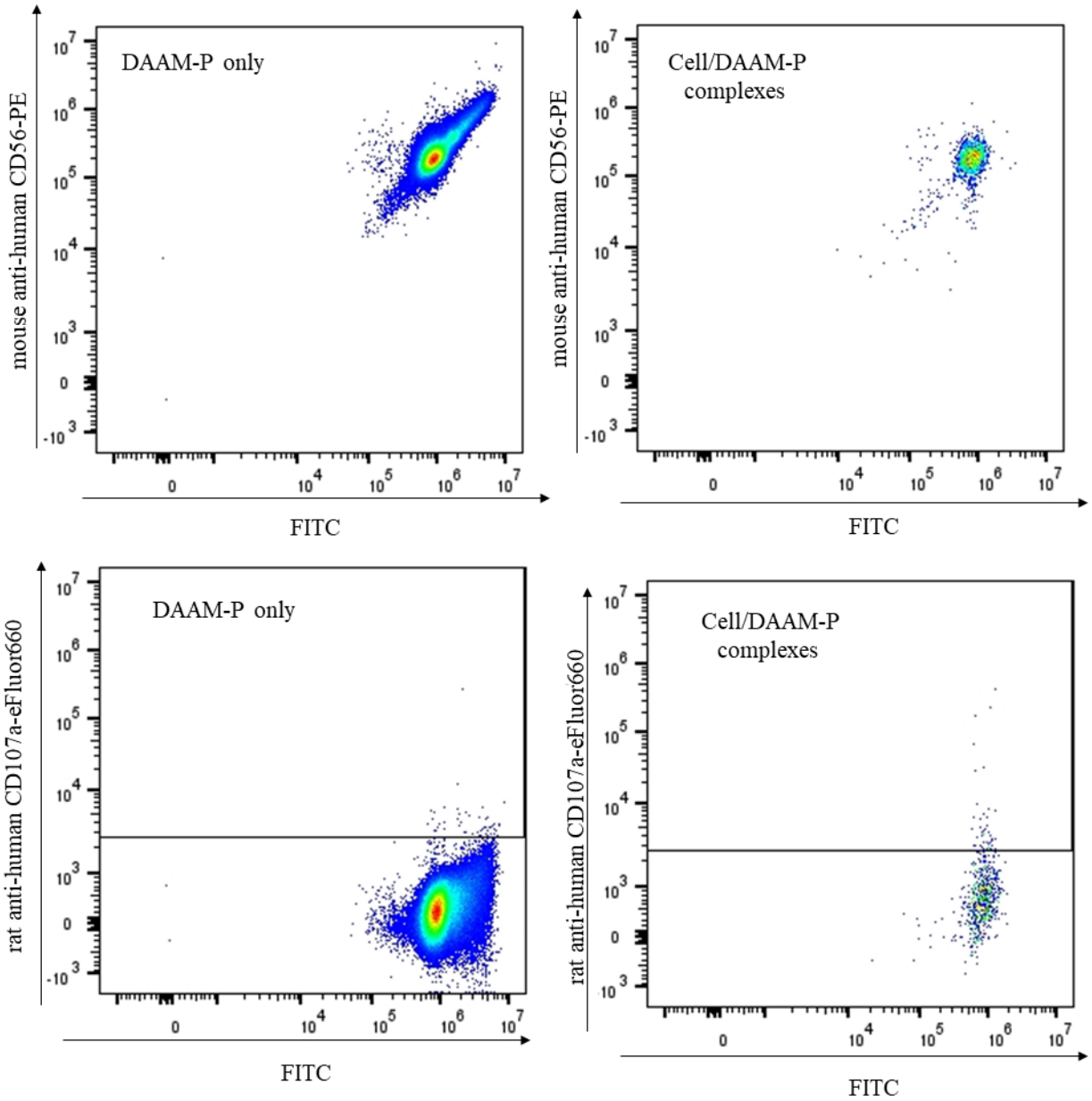

Figure 3. Staining of protein A functionalized DAAM-Ps with mouse vs rat antibodies. DAAM-Ps were functionalized with FITC-cadaverine and protein A and then incubated with either mouse anti-human CD56-PE or rat anti-human CD107a-eFluor660 antibodies alongside samples with PBMCs for 4h. Top left: protein A DAAM-Ps stained with anti-human CD56-PE Top right: lymphocyte/DAAM-P complexes stained with mouse anti-human CD56-PE. Bottom left: protein A DAAM-Ps stained with rat anti-CD107a-eFluor660 antibodies. Bottom right: lymphocyte/DAAM-P complexes stained with rat anti-CD107a-eFluor660 antibodies.

3.3. Surface expression of receptors on KHYG-1 cells

Surface expression of target receptors on KHYG-1 cells, a human NK cell line, was assessed using receptor-specific antibodies and MICA-Fc recombinant protein. Anti-LFA-1, anti-NKp30 and anti-NKp46 antibodies were used to check for the corresponding receptors and detected using secondary antibodies conjugated with AlexaFluor 488. MICA-Fc, a recombinant protein containing a human Fc domain, was used for NKG2D detection together with a secondary anti-human antibody conjugated with AlexaFluor 488. All primary antibodies and MICA-Fc were titrated prior to the final experiment. Samples with cells only and containing cells with secondary antibodies were used as controls. All samples were measured on a flow cytometer at 488 nm. All receptors were successfully detected, with a significant increase in fluorescent signal compared to control (**Figure 4**). Although signal from NKG2D and NKp46 was very low, over 10 fold lower than NKp30, which is suggestive of lower expression of these receptors, there was still an increase in fluorescence in comparison with secondary antibody control and a visible population shift when compared to control (**Figure S1**). LFA-1 integrin showed the highest signal with a 4-16 fold difference in fluorescence intensity in comparison to the other receptors **(Figure 4**).

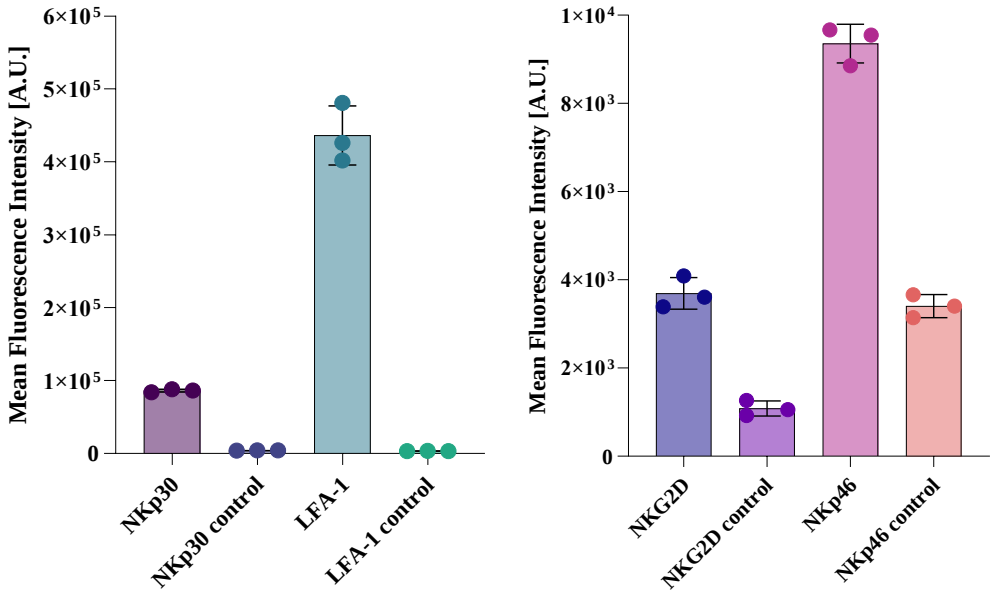

Figure 4. Surface expression of target receptors. Receptors were stained using specific antibodies, except for NKG2D which was detected with MICA-Fc recombinant protein, and secondary antibodies conjugated with AlexaFluor 488. The following concentrations were used for this experiment, determined previously via titration: 5 µg/ml anti-LFA-1, 10 µg/ml anti-NKp46, 1 µg/ml anti-NKp30, 10 µg/ml MICA-Fc. Control samples represent cells incubated only with corresponding secondary antibodies. All samples were done in triplicate and corrected for background from cells' autofluorescence which equalled $5x10^3$. Error bars represent standard deviations in between replicates.

3.4. Immune synapse formation in NK cell activation assays

3.4.1. Role of LFA-1 integrin in IS formation

To trigger LFA-1 mediated immune synapse formation DAAM-Ps (5 kPa, 14,7µm) were functionalized with FITC-cadaverine and coupled with anti-LFA-1 antibodies at concentrations ranging from 0,25 to 25 µg/ml. DAAM-Ps were incubated at a 2:1 ratio with KHYG-1 cells, while DAAM-Ps without anti-LFA-1 were used as control. IS formation, represented by complex formation of NK cells with DAAM-Ps, was subsequently assessed via flowcytometry at 488nm after 15, 30 and 60 min. Cells themselves were identified based on their scattering properties, since their scattering was higher than the DAAM-Ps with low refractive index. Cell/DAAM-P complex formation was assessed by the percentage of cells that emitted a fluorescent signal at a level corresponding to FITC from functionalized DAAM-Ps (**Figure S2**). High levels of complex formation were observed in all samples when compared to negative

control, with the highest outcome registered amounting to 78% of KHYG-1 cells engaging in complexes with DAAM-Ps (**Figure 5**). The highest cell/DAAM-P complex formation was observed after 15 and 30 min, which significantly decreased after 1h, suggesting that KHYG-1 cells can release their targets after prolonged exposure. The number of cell/DAAM-P complexes rose with the increase in anti-LFA-1 concentration until it reached a plateau at 0,8-2,5 µg/ml and subsequently decreased above 2,5 µg/ml. With this method, an optimal concentration for LFA-1 mediated immune synapse formation was determined at 2,5 µg/ml.

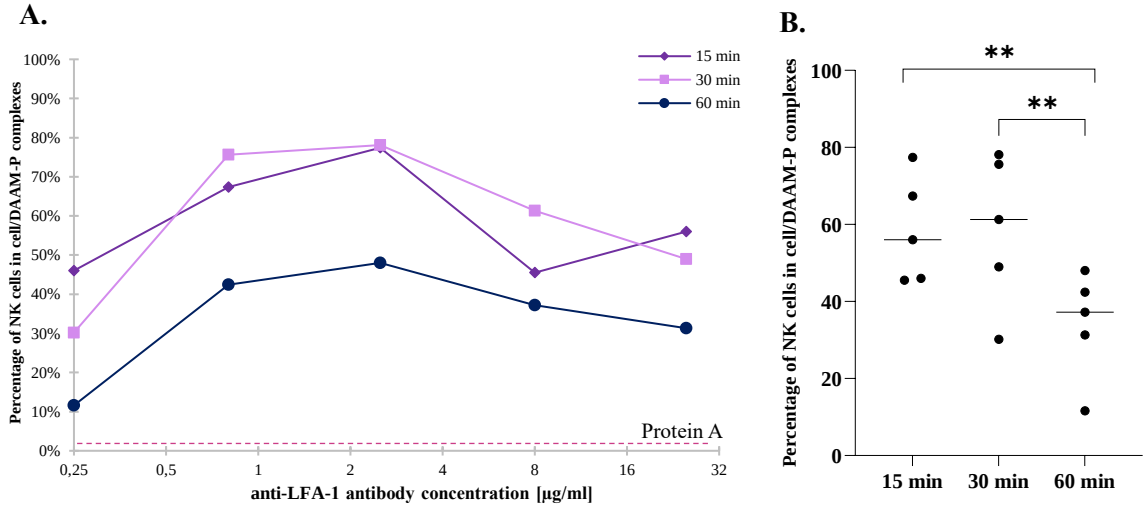

Figure 5. Cell/DAAM-P complex formation upon crosslinking of LFA-1 integrin. DAAM-Ps functionalized with FITC-cadaverine and protein A and then coupled with anti-LFA-1 antibodies at concentrations between 0,25 and 25 µg/ml. **A.** Complex formation with the functionalized DAAM-P was monitored after 15, 30 min and 1h via flowcytometry. DAAM-Ps functionalized with protein A but not coupled with anti-LFA-1 antibodies were used as control to determine the baseline (dotted line). **B.** Complex formation with the functionalized DAAM-Ps after 15, 30 and 60 min. Statistical significance of differences between time points was calculated with a paired t-test. **p<0,005, for 15-30 min: p=0,95.

3.4.2. Role of NKp30 receptor in IS formation

To trigger NKp30-mediated immune synapse formation DAAM-Ps were coupled with anti-NKp30 antibodies or with anti-NKp30 and anti-LFA-1 antibodies at varying concentrations. Cell/DAAM-P complex formation was assessed in the same manner as in triggering LFA-1-mediated IS formation (paragraph 3.4.1.) In the samples where only NKp30 was activated with no LFA-1 co-stimulation, no cell/DAAM-P complex formation was observed at any of the measured time points when compared to control (**Figure 6A**). When additional anti-LFA-1 antibodies were used at an optimal concentration of 2,5 µg/ml with varying concentrations of anti-NKp30, high level of interactions between cells and DAAM-Ps was observed in all samples (**Figure 6B**). However, there was no visible effect of NKp30 targeting as the level of complex formation remained constant around 50-70% independent of anti-NKp30 concentration. However, a decrease in anti-LFA-1 concentration to a suboptimal 0,25 µg/ml resulted in a clear effect of NKp30 stimulation (**Figure 6C**), with the number of cell/DAAM-P complexes increasing with the rise of anti-NKp30 concentration, likely reflecting the role of this receptor in IS formation. A dose-dependent response was observed, with the highest level of interactions observed (50% after 15 min) at the highest anti-NKp30 concentration (25 µg/ml). Similarly to activation of LFA-1 only, complex formation was the lowest after 60 min, possibly indicating that NK cells release their targets after prolonged exposure. Interestingly, in case of NKp30 stimulation the peak was observed after 15 min instead of 30 min after only LFA-1 stimulation. Notably, there was a noticeable inconsistency with the number of cell/DAAM-P complexes observed at a concentration of 0,25 µg/ml of anti-LFA-1 antibodies between experiments. When only LFA-1 was activated, a range of 10-46% of complex formation was measured at different time points (**Figure 5**). On the other hand, with the addition of anti-NKp30 at the same concentration of 0,25 µg/ml anti-LFA-1 no complexes were observed and only reached the 40% with anti-NKp30 concentrations of >8 µg/ml (**Figure 6C**). Nevertheless, these observations likely indicate that NKp30 contributes to IS formation in NK cells when combined with suboptimal LFA-1 co-stimulation.

A.

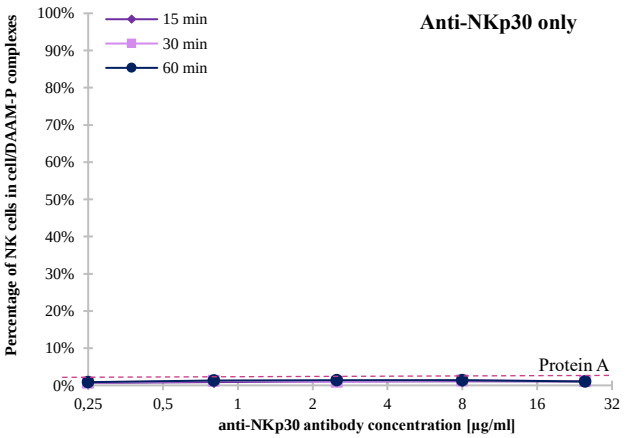

B.

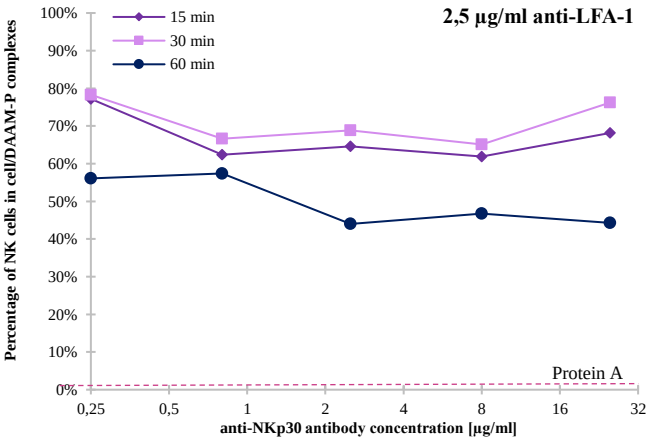

C.

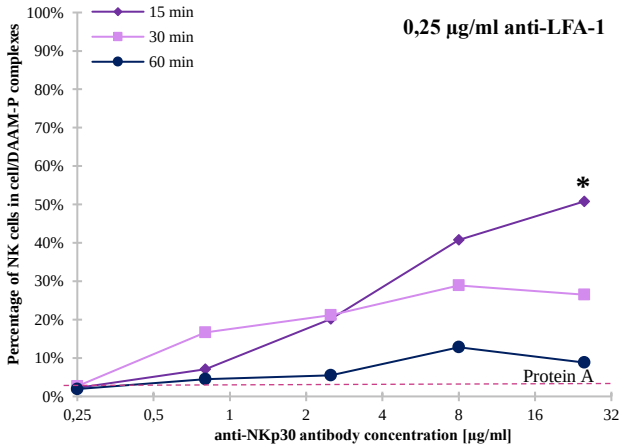

D.

Condition	Time point	Correlation coefficient	p value
Anti-NKp30 only	15 min	0,7	0,23
	30 min	0,5	0,45
	60 min	0,4	0,52
Anti-NKp30 with 2,5 µg/ml anti-LFA-1	15 min	-0,3	0,68
	30 min	-0,3	0,68
	60 min	-0,6	0,35
Anti-NKp30 with 0,25 µg/ml anti-LFA-1	15 min	1	0,017*
	30 min	0,9	0,08
	60 min	0,9	0,08

Figure 6. Cell/DAAM-P complex formation upon activation of NKp30 receptor with and without LFA-1 co-stimulation. **A.** DAAM-Ps functionalized with FITC-cadaverine and protein A and then coupled with anti-NKp30 antibodies at concentrations between 0,25 and 25 µg/ml. **B.** DAAM-Ps functionalized with FITC-cadaverine and protein A and then coupled with anti-LFA-1 antibodies at 2,5 µg/ml and anti-NKp30 antibodies at concentrations between 0,25 and 25 µg/ml. **C.** DAAM-Ps functionalized with FITC-cadaverine and protein A and then coupled with anti-LFA-1 antibodies at 0,25 µg/ml and anti-NKp30 antibodies at concentrations between 0,25 and 25 µg/ml. Complex formation with the functionalized DAAM-Ps was monitored after 15, 30 min and 1h. DAAM-P functionalized with protein A but not coupled with anti-NKp30 antibodies were used as control (dotted line). **D.** Spearman's correlation coefficient of anti-NKp30 concentration and percentage of cell/DAAM-P complex formation at different time points with corresponding p values, min = minutes.

3.5. Activation of LFA-1 and NKp30 on PBMCs with CD107a degranulation marker

To validate our method of triggering complex formation in primary cells and to test the effect of different conditions on NK cell degranulation we used PBMCs and the degranulation marker CD107a. DAAM particles were coupled with anti-LFA-1 antibodies at 2,5 and 0,25 µg/ml alone or with both 25 µg/ml anti-NKp30 and 0,25 µg/ml anti-LFA-1. PBMCs were incubated with the functionalized DAAM-Ps at a 1:2 ratio for 30 min and 4 hours with the addition of anti-CD107a-eFluor660 antibodies. DAAM-Ps with protein A were used as control to determine the baseline number of interactions. Protein A DAAM-Ps without cells were included as an additional control for non-specific binding of anti-CD107a-eFluor660 antibodies. PMA and ionomycin stimulation, agents known to cause NK cell degranulation (Shabrish et al., 2016), were used as positive control. All samples were analysed via flow cytometry. Live lymphocytes were selected based on their scattering properties and the 7-AAD live/dead marker (**Figure S3**). NK cells could unfortunately not be separated from other lymphocytes due to unspecific binding of the anti-human CD56-PE antibody to protein A on DAAM-Ps (paragraph 3.2). Based on FITC signal, complex formation of the live lymphocytes with DAAM-Ps was analysed together with the expression of degranulation marker CD107a. In complexes, CD107a signal was corrected for unspecific antibody binding to protein A on DAAM-Ps. The highest cell/DAAM-P complex formation was observed at 14% after 30 min when higher anti-LFA-1 concentration was used. The amount of interactions drastically decreased after 4h (**Figure 7A**). In contrast, both low anti-LFA-1 and combined

anti-LFA-1 and anti-NKp30 showed low complex formation after 30 minutes (<2%), but an increase in complex formation after 4 hours to 5% and 9%, respectively. This could indicate that an optimum anti-LFA-1 concentration for triggering IS formation at different time points in primary lymphocytes differs from the KHYG-1 cell line. However, this experiment was only carried out in a single repeat and therefore these results can only be taken as an indication of possible trends.

When measuring degranulation, it was surprising that the negative control, protein A DAAM-Ps also showed degranulation after 30 min. However, this measurement was based on extremely few cells as complex formation was below 0,5%, as also clear from the large error on this measurement (**Figure 7B)**. Complexes formed by LFA-1 targeting alone showed almost no CD107a expression after 30 min when corrected for unspecific antibody binding to DAAM-P (**Figure 7B**), indicating that LFA-1 stimulation alone was insufficient for degranulation. When co-stimulation of NKp30 was included CD107a expression was observed and was higher than in LFA-1-only samples at 30 min. Surprisingly, after 4 hours, low, but not high, anti-LFA-1 concentration resulted in degranulation, which was just as high as degranulation of cells stimulated with both anti-LFA-1 and anti-NKp30. A similar trend could be observed when degranulation of all lymphocytes (also those not in a complex) was measured, with combined NKp30 and LFA-1 activation, as well as LFA-1 stimulation at a low concentration, resulting in the highest CD107a signal (**Figure S4**). It is important to point out that we saw a 50% drop in cell viability after 4h incubation and an overall lower number of events in samples measured at that time point, which could affect the acquired results.

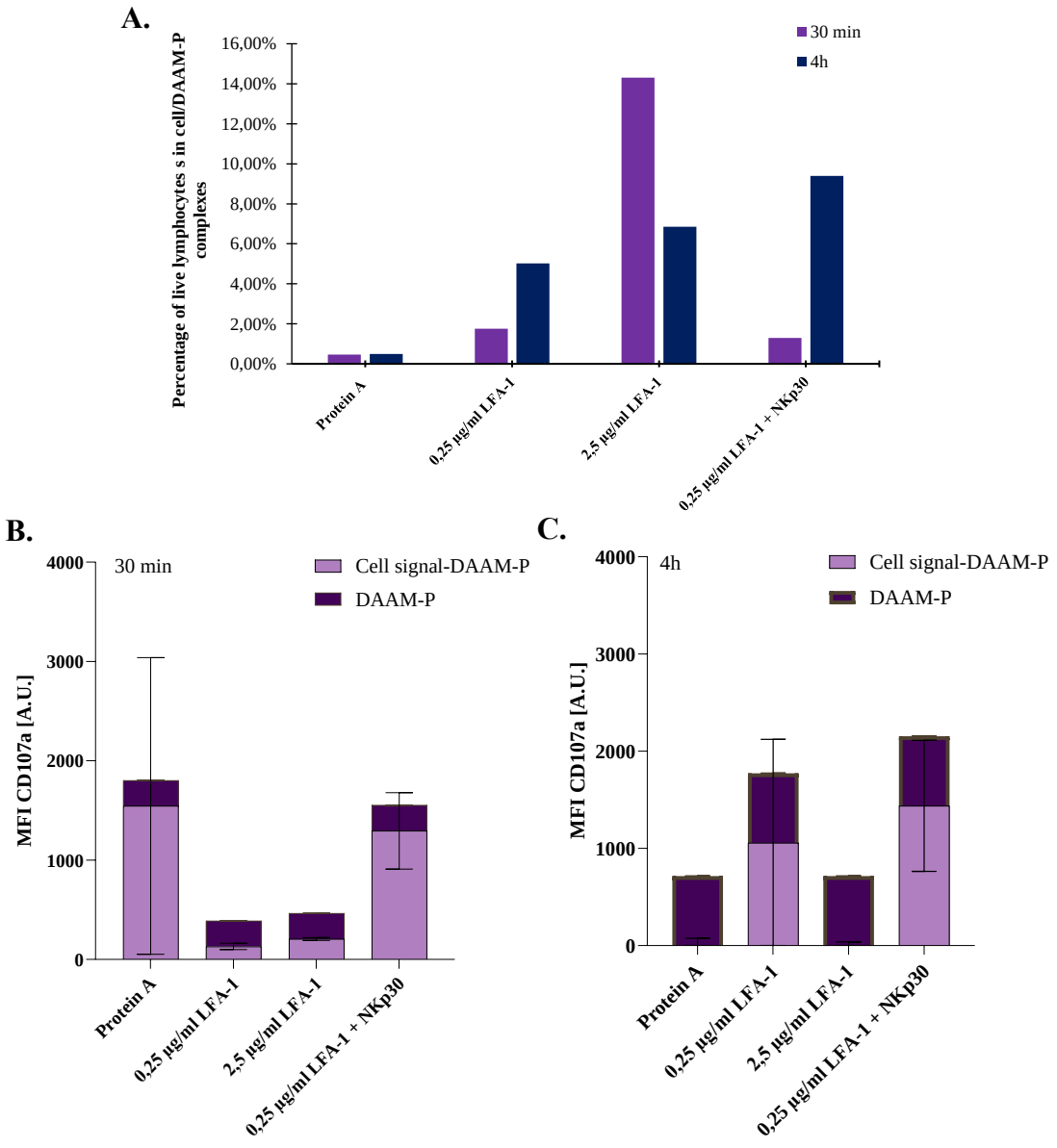

Figure 7. Lymphocyte activation in PBMC activation assay. PBMCs were incubated with DAAM-Ps functionalized with FITC-cadaverine, protein A and anti-LFA-1 antibodies at different concentrations or anti-NKp30 antibodies at 25 µg/ml and anti-LFA-1 at 0,25 µg/ml for 30 min and 4h. Protein A DAAM-P without antibodies were used as control. Live lymphocytes were selected based on FSC, SSC and 7-AAD marker. **A.** Lymphocyte/DAAM-P complex formation after 30 min and 4h of incubation. **B.** CD107a degranulation marker expression of live lymphocytes in cell/DAAM-P complexes detected with rat anti-CD107a-eFluor660 antibodies after 30 min and 4h (**C.**). Background signal from DAAM-P was subtracted from each sample and is indicated on graph. Error bars represent standard error of the mean (SEM) of the anti-CD107-eFluor660 signal in a single sample.

3.6. Imaging receptor-dependent NK cell synapse formation

KHYG-1 are suspension cells and therefore cell/DAAM-P complexes need to be immobilized prior to high-resolution imaging. Multiple approaches were previously used, including attaching cells with poly-L-lysine to the bottom of a glass plate and attaching DAAM-P to a plate coated with BSA and anti-BSA antibodies. However, these methods came with severe disadvantages. Methods including cell or DAAM-P attachment to a surface were considered non-favourable due to previous reports of severe deformations either in the NK cell cytoskeletal structure or in DAAM-P shape from the additional interactions with a glass surface and coating agent (de Jesus et al., 2023; Niek Frijlink, 2023). Additionally, using a plate coated with BSA and antibodies could result in unspecific interactions between the IgGs and Fc receptor on NK cells. Hence, we tried a new approach including suspending complexes in agarose, as it offered the least interruptions to imaging synapse morphology.

3.6.1. Optimising cell immobilisation and staining method

As a first step towards imaging NK cell/DAAM-P complexes in agarose gel 500 000 KHYG-1 cells were incubated with DAAM-Ps in a 1:2 ratio. After activation, cells were fixated with formaldehyde in an Eppendorf tube. The cell membrane was then permeabilized with Triton X-100 and actin was stained with phalloidin conjugated with AlexaFluor488. With this approach cells were no longer visible in the pellet after permeabilization and there was no observable sample after suspending in agarose, likely due to the change in hydrophobicity from permeabilization causing the cells to adhere to tube walls. Two different strategies were then considered to avoid the effect of permeabilization on the ability to pellet the cells. A schematic representation of the experimental setup can be seen in **Figure 8A**. First, samples were directly suspended in agarose after fixation with formaldehyde and then permeabilized and stained within the gel to avoid the need for centrifugation. Second, 30 mg/ml BSA was added to all solutions used after fixation to prevent cells adhering to tube walls. They were then suspended in agarose after permeabilization and staining in Eppendorf tubes. In both of these methods two different sample to agarose ratios were included: 1:1 and 1:9. Samples were observed in a confocal microscope at 488 and 561 nm. Strikingly, all these strategies led to many observable cell/DAAM-P interactions.

Comparing the sample preparation strategies, samples stained within agarose resulted in more background signal from phalloidin than the samples stained in tubes (**Figure 8**). The background was particularly prominent when cells were stained within a bigger volume of agarose (1:9 sample to agarose ratio) **(Figure 8C**). To more accurately compare the differences between these staining methods, signal to noise ratios (SNR) of single cells were analysed. To that end, based on line profiles created in ImageJ, mean SNR was calculated or each condition from 10 different cells at multiple locations within a well. Samples that were stained in Eppendorf tubes resulted in a significantly higher SNR than those stained within a bigger volume of agarose (**Figure 9**). When staining cells within agarose the phalloidin that diffused into the gel overnight could not be properly washed out, which can be seen as an increased background noise across multiple locations within one sample. This effect was, as expected, significantly higher in a thicker layer of agarose than when less agarose was used for suspension. When staining in tube with a subsequent embedding in the gel, different agarose dilutions had no significant effect. There was also no notable difference between staining within a thin layer of agarose and staining in tube with a 1:9 dilution. However, staining in tube with a 1:1 sample to agarose ratio resulted in less noise than when staining within agarose. Overall, while all of these fixing and staining strategies, could

work, high SNR and relatively short incubation time makes staining in tube and suspending the samples in agarose at a 1:9 dilution the preferred method.

Although many cells were interacting with more than one DAAM-P, which is consistent from previous flow cytometry experiments (**Figure S2**) and the density of events in all samples was lower than desirable, which could easily be optimized through increasing the cell/DAAM-P concentration and including a filtering step, this protocol should allow for easily imaging DAAM-P interactions in high resolution.

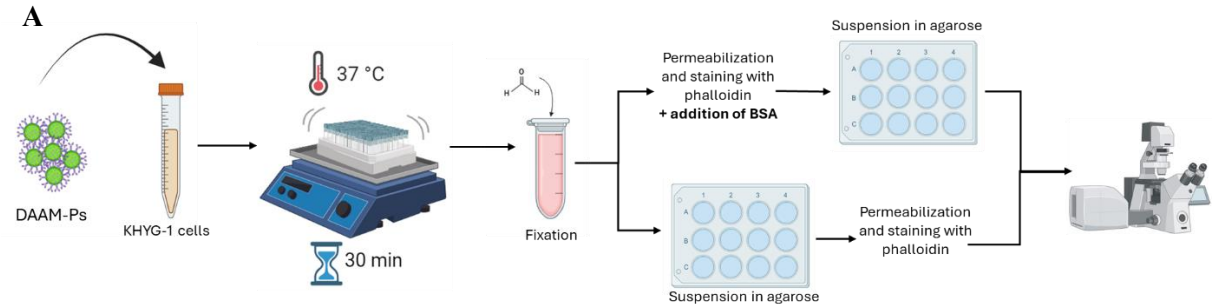

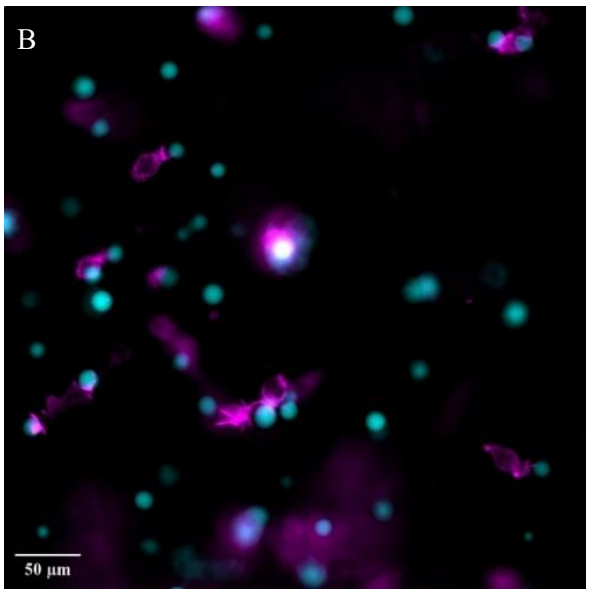

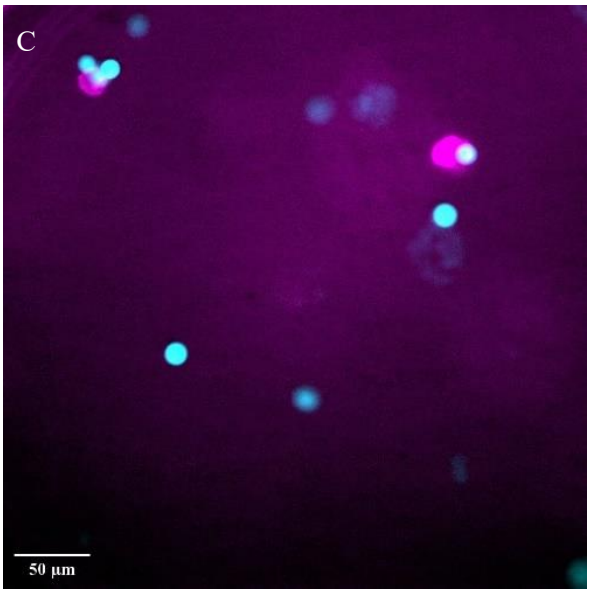

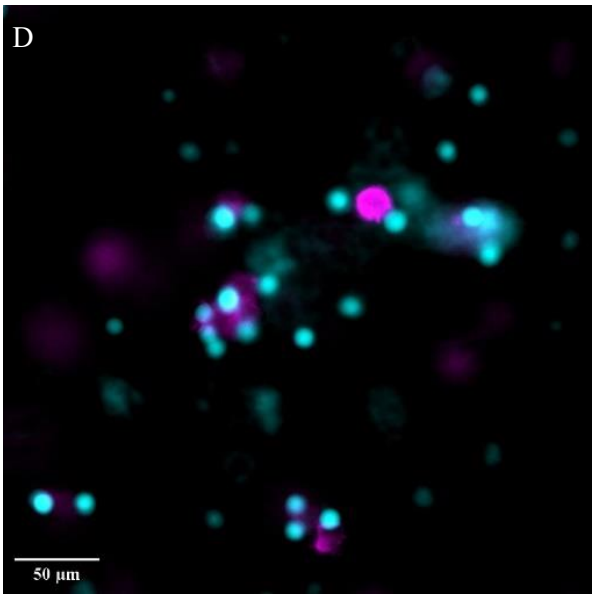

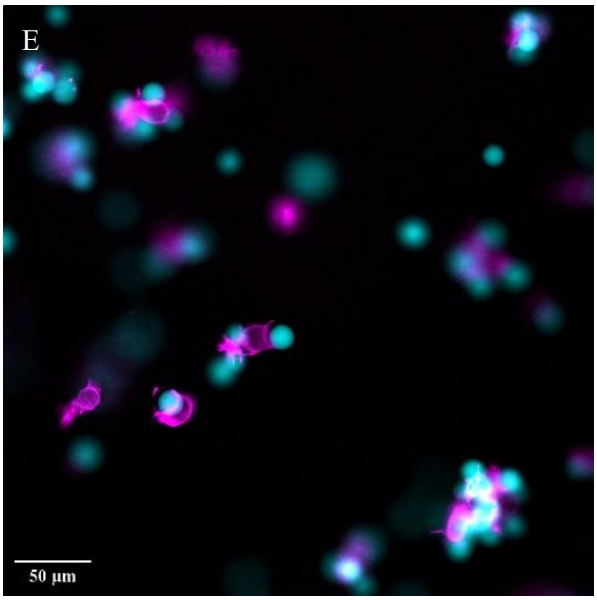

Figure 8. Comparison of different immobilization and staining methods for imaging NK cell/DAAM-P complexes. Pictures taken with confocal microscope showing KHYG-1 cells (magenta) and DAAM-P (cyan) functionalized with protein A, TMR-cadaverine and 2,5 µg/ml anti-LFA-1 antibodies, incubated with cells for 30 min. $5x10^5$ KHYG-1 cells and 10^6 DAAM-P used in each sample. **A.** Schematic representation of the experimental setup. **B.** Sample diluted 1:1 with 1% agarose and stained after immobilization in the gel. **C.** Sample diluted 1:9 with 0,5% agarose and stained after immobilization in the gel. **D.** Sample stained in Eppendorf tube and then immobilized in gel, diluted 1:1 with 1% agarose. **E** Sample stained in Eppendorf tube and then immobilized in gel, diluted 1:9 with 0,5% agarose.

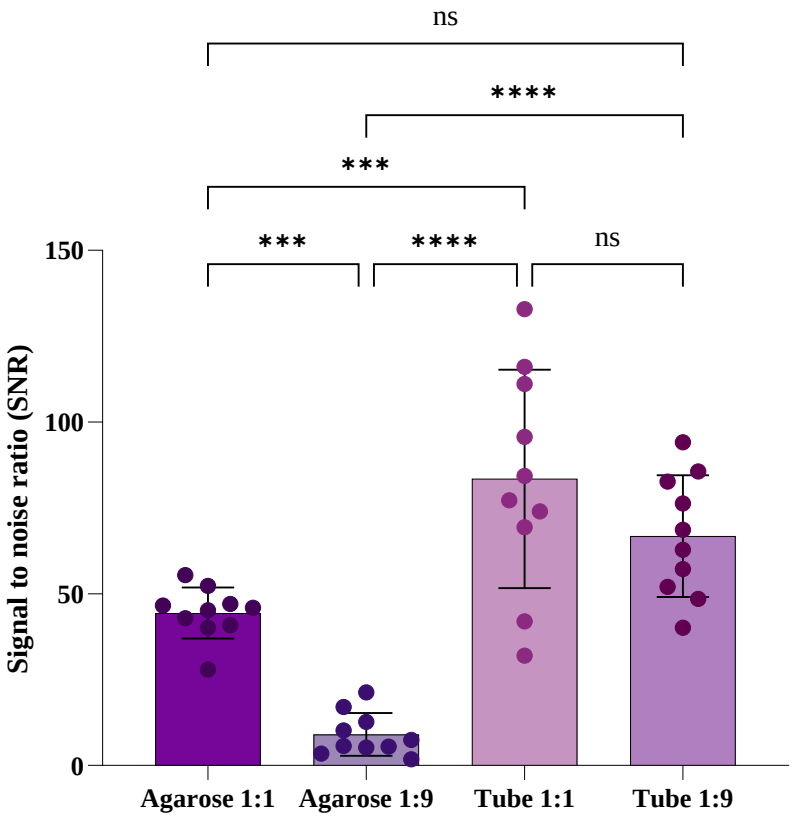

Figure 9. Comparison of signal-to-noise ratios (SNRs) in different NK cell/DAAM-P imaging methods. Samples were either stained after embedding in the gel ("Agarose") or in Eppendorf tubes ("Tube") and subsequently suspended in agarose. Agarose was added to samples in a 1:9 or 1:1 samples to agarose ratio. SNRs were determined by subtracting the mean signal of the background from mean of single cells, divided by standard deviation of background signal. Calculations were repeated for 10 cells in each condition and statistical significance was analysed with a one-way ANOVA in GraphPad. ****p< 0,0001, ns – not significant. Error bars represent standard deviations in between replicates.

3.6.2. IS morphology in KHYG-1 cells upon LFA-1 engagement

Lastly, we decided to magnify a few representative NK cell/DAAM-P complexes from the imaged samples to try and visualize IS morphology. Ideally, this would have been done with high resolution microscopy, however, unfortunately, this was not an option due to time restraints and technical problems with the KHYG-1 cell line. Nevertheless, we obtained some intriguing images of cells interacting with DAAM-Ps functionalized with 2,5 µg/ml anti-LFA-1. We observed KHYG-1 cells form an enriched actin ring at the point of interaction with DAAM-Ps with a less actin-dense middle, indicating IS formation (**Figure 10C**). Surprisingly, multiple cells formed "finger-like" actin protrusions, which differed from the typical IS morphology observed in CTLs and the phagocytic cup in macrophages (Jesus et al., 2023; Vorselen et al., 2020). Additionally, we saw cells extending their actin network to interact with multiple DAAM-Ps at once (**Figure 10D**), as well as cells that seemed to have protruded around the whole particle (**Figure 10A**). Overall, these intriguing observations of the IS structure make for an interesting reference point for future high-resolution imaging studies.

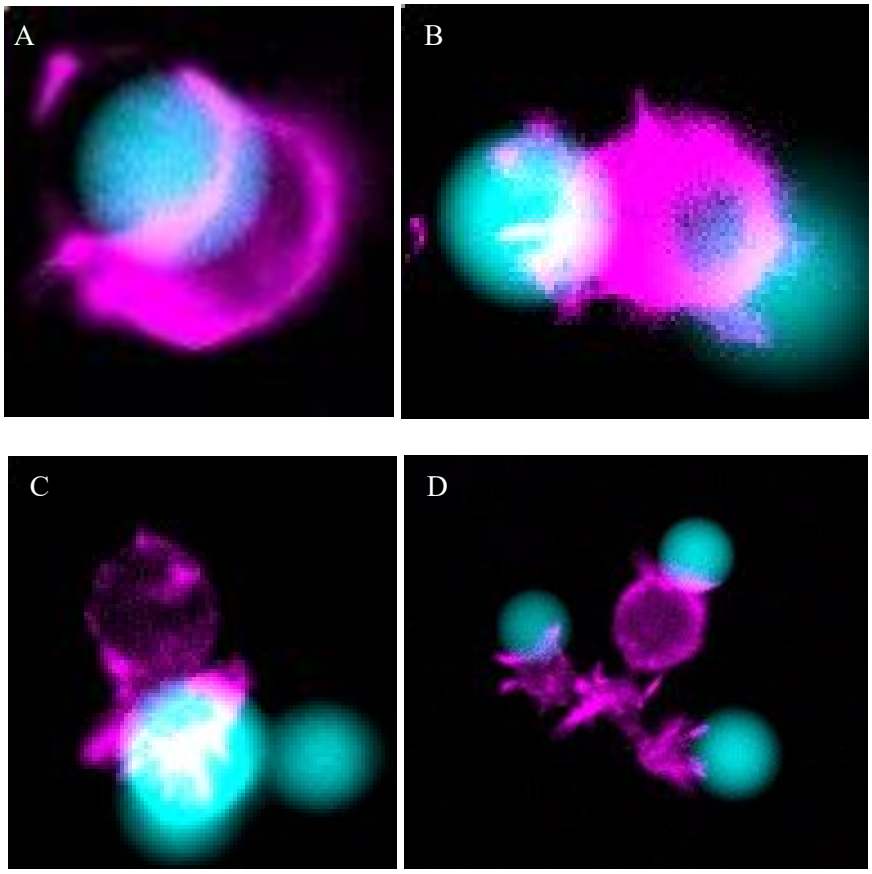

Figure 10. Magnified images of NK cell/DAAM-P complexes. DAAM-Ps (cyan) were functionalized with TMR-cadaverine, protein A and anti-LFA-1 antibodies at 2,5 µg/ml and incubated with KHYG-1 cells (magenta) for 30 min. Filamentous actin was stained with phalloidin-Alexa Fluor 488. Samples were imaged in a Nikon Ti2 microscope with LED light and a 40x lens, single cell/DAAM-P complexes were chosen and magnified.

4. Discussion

Although NK cells play a vital role in the immune response against pathogens and cancer, many questions remain on how they form immune synapses with their targets and how different receptors contribute to this process. Here, we developed and optimised a method to study the IS of NK cells using DAAM-Ps functionalized with protein A and receptor-specific antibodies. With this method, we illustrated the importance of LFA-1 integrin activation for adhesion to the target and IS formation. We also demonstrated the role of NKp30 receptor in supporting that process and in promoting degranulation. With this methodology, we expect that future studies can further expand our understanding of how different receptors affect NK cell cytotoxic activity and implement that knowledge in developing new NK cell-based immunotherapies.

4.1. Optimizing protein A DAAM-Ps as a flexible platform for triggering NK cell responses

To trigger IS formation in NK cells we used 14,7 μm, 5 kPa DAAM-Ps, to as closely as possible mimic the physical properties of cells. To conjugate DAAM-Ps with specific antibodies we first functionalized them with protein A. Protein A is widely used for antibody purification in affinity chromatography thanks to its IgG-binding ability (Hjelm et al., 1972). It non-covalently binds many classes of mammalian antibodies from different species via hydrophobic interactions between protein A and the Fc domain of antibodies (Zarrineh et al., 2020). Here, we use that characteristic to conjugate DAAM-Ps with antibodies while leaving their Fab region exposed for interactions with specific receptors on the surface of NK cells (**Figure 2A**). This method of binding IgGs to DAAM-Ps presents a powerful and flexible functionalization strategy. It can be easily adapted to trigger alternative receptors, or for triggering other (immune) cells. Compared to alternative functionalization strategies, such as using streptavidin, it does not require biotinylated antibodies and allows for direct conjugation of most IgGs and chimeric proteins containing an Fc domain, saving both time and resources. Additionally, protein A DAAM-Ps remain stable for at least 7 weeks after functionalization (**Figure S5**), which means that they can be prepared beforehand in bigger batches and conjugated with specific antibodies as needed.

4.1.1. Antibody binding to protein A on DAAM-P is pH dependent

In chromatography, the binding of antibodies to protein A is typically done at neutral or alkaline pH and elution is performed by lowering the pH to alkaline values. Therefore, we assumed that pH would also highly affect the binding efficiency of IgGs to protein A on DAAM-Ps. Since the binding efficiency and optimal pH depends on the species of origin and subclass of the antibody (Hober et al., 2007), we used rabbit IgGs, as they are most representative for antibodies used in future experiments. Of the different buffers (pH 7.5 – 9) tested, we found that binding of antibodies to DAAM-Ps was most efficient at pH 9. This yielded a 14% increase in efficiency compared to previous experiments performed at pH 7.5 (**Figure 2**). This means that lower IgG concentrations can be used to achieve the same IgG coating density, and notably lowers the price of future experiments involving antibody-coupled DAAM-Ps, and broadens their usage in cell activation assays. Since most antibody species and subclasses, including mouse (Bio-Rad Laboratories, 2016), bind more efficiently at higher pH, I expect these optimized conditions to lead to improved binding more generally. Moreover, this protocol has also been successfully implemented in macrophage activation assays. However, it would be advisable to determine the optimum pH experimentally when using antibodies of distinct binding characteristics (*e.g.* llama IgG), or when antibody amounts are limited.

4.1.2 Antibodies of rat origin enable joined use of protein A DAAM-Ps with cellular stains

A disadvantage of using DAAM-Ps functionalized with protein A, is it creates a limitation for any additional antibody-based staining done during an experiment, where the risk is present that the protein A DAAM-Ps strongly absorb these antibodies. Most antibodies will bind to excess protein A on DAAM-Ps, generating false-positive readouts for cells in cell/DAAM-P complexes. To address this, we explored

using antibodies from different host species, which differ in their binding efficiency to protein A (Hober et al., 2007). Specifically, in affinity chromatography rat antibodies were shown to have low binding efficiency, and have to be purified with protein G instead (New England Biolabs, 2024). Indeed, we showed that mouse antibodies bind very efficiently to protein A on DAAM-Ps, generating background that prevents from distinguishing between positive and negative cell populations (**Figure 3**). Importantly, this was not the case for rat antibodies, which bound to DAAM-Ps inefficiently, resulting in little background. With these antibodies a distinct positive population of cells could be identified, and shows that use of protein A DAAM-Ps can be effectively combined with cellular staining.

4.2. Suspension in agarose of cell/DAAM-P complexes is a promising method for high resolution imaging of the IS

High resolution imaging of IS morphology in suspension cells has faced multiple obstacles in the past. Most detailed IS imaging studies in NK cells and other lymphocytes have used total internal reflection fluorescence (TIRF) microscopy (Ambrose et al., 2020; Carisey et al., 2018), which requires the observations to be made on a glass surface. While informative, imaging on an extremely rigid and flat surface differs greatly from physiological conditions in which lymphocytes are interacting with round cells of 0,1-10 kPa in rigidity (Cross et al., 2007). As it has been shown that target rigidity affects actin dynamics in T cells and fibroblasts (Gupta et al., 2015; Hui et al., 2015), and the same is speculated for NK cells, improved imaging methodologies are imperative to accurately depict IS morphology. Friedman et al. (2021) have attempted to use sodium alginate beads coated with poly-L-lysine and antibodies as three-dimensional targets to image the IS in NK cells. However, this methodology was limited to beads of 9-254 kPa in stiffness, missing the most relevant stiffness range for NK cells targets (0.1 – 10 kPa). Moreover, high variability between beads in rigidity (±7 kPa for 9 kPa beads), shape and diameter, leads to reduced reproducibility. Finally, this approach does not allow to measure forces exerted by NK cells on their targets.

In this study, we used DAAM-Ps of adjustable rigidity between 0,3 and 10 kPa, which mimic the physical characteristics of cells. DAAM-Ps allow for detailed visualisation of surrounding cellular structures due to their low refractive index, as well as for calculation of forces exerted by cells on their targets (Vorselen et al., 2020). DAAM-Ps have been recently used for a detailed topographical analysis of the IS in T cells by de Jesus et al. (2023). Their approach for high resolution imaging of suspension cells included attaching DAAM-Ps functionalized with streptavidin and biotinylated ICAM-1 to a plate coated with anti-ICAM-1 antibodies. While it allowed for detailed imaging, any method including attachment of soft DAAM-Ps to a flat surface leads to the deformation of their structure at the adhesion point and subsequently greatly impairs the ability to measure forces (de Jesus et al., 2023; Niek Frijlink, 2023). Additionally, in NK cells, the antibodies used to coat a plate and attach DAAM-P could lead to non-specific activation of the CD16 receptor, which recognizes the Fc region of IgG (Capuano et al., 2021).

Here, we propose a novel method for high resolution imaging for IS morphology that constitutes suspending preformed cell/DAAM-P complexes in agarose gel. Embedding in agarose has been successfully used before as a method for single-molecule light-sheet imaging of the organization of membrane proteins in T cells (Ponjavic et al., 2018). To adapt this technique to imaging NK cell IS we tried multiple different staining and suspension approaches. We showed that both staining fixated cell/DAAM-P complexes with phalloidin in suspension and within the gel itself resulted in clear images of complex formation (**Figure 8**). Only staining within a larger volume of agarose produced significantly more noise from undiffused phalloidin and was discarded as least optimal, while all other approaches could be considered based on specific experimental setups (**Figure 9**). Staining cells in suspension and embedding them in agarose at a 1:9 ratio has experimental advantages: It includes a shorter incubation time than staining within agarose and a bigger dilution is easier to handle than a small volume of agarose, which solidifies within seconds. This innovative method is generalizable, and allows for high resolution IS imaging and force detection not only in NK cells but also in other lymphocytes, and possibly can be extended to live cells, as it offers no disruptions to the physical structure of DAAM-Ps or to the dynamics

of the cytoskeleton. Future studies should focus on optimizing detailed embedding protocol, possibly considering increasing the concentration of cell/DAAM-P complexes and including a filtration step to remove large cell/DAAM-P clusters. Additionally, using low-melting point agarose could be considered in live cell imaging to observe detailed changes in IS over time under different activating/inhibitory conditions.

4.3. Complex formation with LFA-1 coupled DAAM-P is inconsistent

Important to point out is the inconsistency of complex formation with DAAM-Ps coupled with anti-LFA-1 antibodies. Our first experiments showed that even at the lowest anti-LFA-1 concentration over 30% of cells interacted with DAAM-P (**Figure 5**). When the same anti-LFA-1 concentration was used together with NKp30 stimulation there was almost no observable IS formation at the lowest anti-NKp30 concentration (**Figure 6**). This discrepancy could be caused by unintentional differences in DAAM-P number during functionalization. We have seen over multiple experiments that even with adequate mixing and pipetting the same volume, the absolute number of DAAM-Ps still varies per sample. When less DAAM-Ps are present, even with the same antibody concentration possibly more IgGs could bind to protein A and effectively increase the number of potential interactions with integrins. This would explain why we see a difference in complex formation between experiments using low but not high anti-LFA-1 concentrations. Cellular variation could also contribute to the observed inconsistency as the KHYG-1 cells are very sensitive to changes in cell density and the concentration at which they were harvested from culture could have possibly influenced their activity. Another reason could lie within the functionalization protocol, where DAAM-Ps are first incubated with anti-LFA-1 and then with anti-NKp30 antibodies. It is possible, that during the second incubation, which includes vigorous mixing for 1h, a part of anit-LFA-1 IgGs detach from protein A, leading to less integrin crosslinking. This could be tested by including an additional control of anti-LFA-1 DAAM-P that are put through a second incubation step without any antibodies and comparing them with DAAM-Ps that were only incubated once. Additionally, counting DAAM-Ps before coupling with IgGs on a flow cytometer instead in a haemocytometer could reduce the error in calculating the final concentration.

4.4. LFA-1 integrin allows for adhesion and IS formation but is insufficient for degranulation

Formation of an immune synapse is a tightly regulated process, requiring engagement of multiple receptors and signalling pathways. Integrins are mechanosensitive receptors, which play a crucial role in the immune system, mediating leukocyte trafficking to lymph nodes, interactions with antigen presenting cells (APCs) and adhesion to target cells (Hynes, 1992). We showed that LFA-1 is highly expressed on KHYG-1 cells (**Figure 4**) and its activation via anti-LFA-1 functionalized DAAM-Ps leads to NK cell/DAAM-P complex formation in ~70% of cells (**Figure 5**). This observation was unique to LFA-1 activation as triggering only NKp30 receptor led to no complex formation (**Figure 6A**). On the other hand, LFA-1 stimulation was insufficient to trigger degranulation in PBMCs after 30 min of incubation (**Figure 7B**). This is consistent with its known role in cell-cell adherence, and role in actin remodelling and cellular contractility in the IS (Long et al., 2013; M. S. Wang et al., 2022). We established an optimum anti-LFA-1 antibody concentration for this method of LFA-1 activation at 2,5 µg/ml, above which, surprisingly, the amount of interactions started to decrease. The reason underlying this oversaturation with anti-LFA-1 is unclear and, to my knowledge, has not been observed before. Firstly, since this experiment was not repeated, it should be confirmed whether this observation is reproducible. Should this effect be reproducible, it could indicate that too much IgG on DAAM-Ps prevents clustering of LFA-1 on the cells. In consequence, this could indicate that overstimulation of the integrin may have a counterintuitive effect of suppressing LFA-1 signalling, which would have to be taken into account in future research on LFA-1 function.

It is also important to mention that antibody binding differs from ligand-receptor interactions. Ligands are typically small peptides ideally suited to bind to the ligand-binding site of the receptor and antibodies bind the receptor via their antigen-binding site. While both can lead to the activation of intracellular

signalling they can differ in functional consequences, it therefore is important to validate these findings using recombinant proteins containing an Fc domain and ICAM-1 ligand.

As we have shown that LFA-1 allows for the formation of the IS in NK cells, upregulation of LFA-1 and ICAM-1 could be considered as a potential therapeutic strategy in NK cell-based immunotherapy. Metformin, a common type 2 diabetes drug, has been shown to increase ICAM-1 expression in leukemic cells, which led to an increase in NK cell killing of cancerous cells, with no effect on non-transformed cells (Allende-Vega et al., 2022). A recent study in CTLs also showed and increased anti-tumour activity in cells with induced LFA-1 overexpression in conjunction with anti-PD-1 therapy both *in vitro* and *in vivo* (Shan et al., 2024). Altogether this conveys the high potential of including the upregulation of integrin interactions in future NK cell-based immunotherapies. However, it should also be taken into account that if our observations on LFA-1 overstimulation are reproducible, upregulation of LFA-1 ligands might only be beneficial until a certain threshold, above which it would be disadvantageous for NK cell activation.

A largely neglected function of integrins in IS formation is mechanotransduction. Activated LFA-1 integrin is coupled to F-actin which allows for the formation of mechanosensitive "catch bonds" with ICAM-1, that in turn enables intracellular transduction of mechanical signals (Huse, 2017; Legate et al., 2009). The actin network in NK cells has been mostly studied as a static scaffold affected by biochemical signalling, while omitting the role of actin dynamics and possible generation of forces that affect cellular activity. In previous studies, Matalon et al. (2018) have shown that actin retrograde flow (ARF), generated by the pushing and pulling forces of actomyosin network, regulates SHP-1 enzyme responsible for NK cell inhibitory response. It shows that the cytoskeleton dynamics have a direct effect on the cell's activity and its response to a potential target. Cytotoxic activity of NK cells is also dependent on target rigidity, with stiffer targets facilitating a stronger response (Friedman et al., 2021). This importance of mechanotransduction is highlighted by the current knowledge on mechanical properties of highly tumorigenic, metastatic cancer cells, which are typically softer than normal cells and non-metastatic tumour cells (Lv et al., 2021). However, little research is done on the effect of existing and emerging immunotherapies on NK cell mechanobiology and it remains unknown to which degree does mechanosensing affect NK cell based therapies. Future research could focus on that aspect of NK cell activity and determine whether they exert physical forces on their targets using the protein A DAAM-P assays established in this study, as well as on the possible role of LFA-1 integrin and target rigidity in that process.

4.5. NKp30 allows for degranulation but requires LFA-1 co-stimulation for successful IS formation

NKp30, one of the natural cytotoxicity receptors (NCRs), is an activating NK cell receptor that recognizes multiple tumour-associated ligands (Brandt et al., 2009). In this study we set out to determine the role of this receptor with and without LFA-1 co-stimulation in IS formation. While NKp30 activation is often analysed in the context of degranulation, there is little research done on its role in the initial stages of establishing a connection with the target. Our results suggest that NKp30 stimulation by itself is not sufficient to trigger complex formation with DAAM-Ps (**Figure 6A**). When combined with LFA-1 co-stimulation at a high anti-LFA-1 concentration no effect of NKp30 activation was seen as the maximum potential of complex formation was reached solely through integrin interactions (**Figure 6B**). However, when we decreased the anti-LFA-1 concentration, NKp30 activation increased complex formation with DAAM-Ps in a dose-dependent manner (**Figure 6C**). This result directly contradicts a study by Wang et al. (2012), who suggested that NKp30 is necessary for degranulation, but not for complex formation. A possible explanation for this discrepancy could be that they used HeLa cells as targets and did not modulate the expression of LFA-1 ligands. As we observed that NKp30 activation only had an effect on cell/DAAM-P complex formation when integrin signalling was limited, likely in their case LFA-1 signalling was sufficient to trigger IS formation without additional co-stimulation.

Contrasting both these, as well as our results Carisey et al. (2018) found that NKp30 activation without LFA-1 co-stimulation was sufficient to induce adhesion and actin remodelling, with LFA-1 activation

resulting in a more stable IS. A possible explanation for this difference in outcome could be that they used an antibody-coated glass slide, which is over a million times more rigid than DAAM-Ps used in our experiments. The high target rigidity, combined with a flat, two-dimensional geometry, most likely increased NK cell activity and non-specific integrin activation even without LFA-1 crosslinking. In line with our results, however, they also observed mature IS formation and degranulation after 30 min, which is consistent with our findings of peak complex formation around 15-30 min. This is noticeably longer than in CTLs, which form a mature IS in under 6 min from activation (Ritter et al., 2015). It also strongly suggests an existence of additional checkpoints during NK cell activation.

Mechanistically, enhanced IS formation upon NKp30 triggering, could be a result of NKp30 stimulating "inside-out" activation of LFA-1. "Inside-out" activation is a process that happens when intracellular signalling triggers conformational changes in integrins that increase their ligand binding affinity (Shi & Shao, 2023). NKp30 is known to trigger many signalling pathways upon activation, which could facilitate this process (Chen et al., 2020). This would be consistent with the observed effect on complex formation only when LFA-1 crosslinking was limited. This shows that while LFA-1 stimulation is necessary for establishing a connection with the target, possibly due to the existence of integrin-dependent mechanical checkpoints (Wang et al., 2022), NKp30 activation also contributes to successful IS formation and maintenance.

We attempted to confirm the observed role of NKp30 and LFA-1 in PBMCs. Unfortunately, due to unspecific binding of the CD56 marker, we could not identify the NK cell population within our samples. However, we saw that over 14% of all live lymphocytes formed complexes with DAAM-Ps functionalized with 2,5 µg/ml anti-LFA-1 after 30 min of incubation (**Figure 7A**). We cannot directly compare this with results from KHYG-1 cells, as some of the DAAM-Ps were being taken up by monocytes, and not just NK cells, but all lymphocytes were included in the calculations. Still, this confirms that our method is applicable to primary cells. We observed an increase in complex formation after 4h of incubation for lower anti-LFA-1 concentration and combined LFA-1 and NKp30 stimulation, which differed from results acquired from the KHYG-1 cells. However, these percentages could be influenced by a drop in cell viability that we saw after 4h and low overall cell numbers, possibly affecting the accuracy of these measurements.

Our results showed higher surface expression of the CD107a degranulation marker in lymphocytes with both LFA-1 and NKp30 stimulation than in those incubated with only anti-LFA-1 DAAM-Ps after 30 min of incubation (**Figure 7B**). This observation coincides with literature, as it is thought, that signals from activating receptors are necessary to initiate MTOC and lytic granule polarisation (Wong & Ding, 2023). Although we saw degranulation in samples stimulated with low anti-LFA-1 concentration after 4h (**Figure 7C**), this observation, similarly to complex formation at this time point, could be deemed unreliable due to low cell numbers and viability. A similar result was observed by Friedman et al. (2021), as they saw an increase in CD107a expression in NK cells with combined LFA-1 and NKp30 activation, compared to only LFA-1. This suggests that indeed, while integrins are necessary for initial adhesion and mechanotransduction, signalling from activating receptors like NKp30 is crucial for the full cytotoxic response. However, it is important to remember that in this test both NK cells and CTLs could have degranulated as CTLs can also express LFA-1 and NKp30 receptors (Correia et al., 2018; Walling & Kim, 2018). To validate these results, this experiment should be repeated using the KHYG-1 cell line or PBMCs with a NK cell marker of rat origin.

This knowledge on the roles of LFA-1 and NKp30 can also be further applied in immunotherapy research. Decreased NKp30 expression on NK cells has been associated with poor outcomes in patients suffering with cervical cancer, while *in vitro* NKp30 activation has been shown to enhance NK cell killing of cervical cancer cells (Guo et al., 2023; Gutierrez-Silerio et al., 2023). However, there is limited research on the therapeutic potential of NKp30. Recently, Klausz et al. (2022) have designed novel NK cell engagers targeting NKp30, which promoted NK cell activity against tumour cells. However, most attempts to utilize NKp30 in immunotherapy have been based on chimeric antigen receptor T cells (CAR-T cells), which have shown promising results *in vivo,* but are associated with concerns regarding the cost of such therapy (Butler et al., 2022; Zhang et al., 2012). A possible alternative could be to design

a bispecific therapeutic antibody that engages both NKp30 and LFA-1 or to consider inducing ICAM-1 expression in conjugation with an NKp30-based therapy for sufficient NK cell activation.

4.6. LFA-1 engagement leads to IS formation of atypical morphology

To gather more insight into the interactions between KHYG-1 cells and DAAM-Ps functionalized with 2,5 µg/ml anti-LFA-1 antibodies, we magnified images obtained from suspending cell/DAAM-P complexes in agarose gel. In these images we observed the cells forming "finger-like" actin protrusions at the IS (**Figure 10**), which differed from IS morphology observed in CTLs and macrophages (Jesus et al., 2023; Vorselen et al., 2020). This atypical structure has been shown before in NK cells upon activation of the NKG2D activating receptor by Niek Frijlink (2023), using a similar protein A DAAM-P-based method. To my knowledge, this has not been observed using more traditional imaging methods, utilising rigid two-dimensional targets. This further supports our proposed method for IS imaging as a promising approach to gaining more understanding of the mechanisms of interactions between NK cells and their targets. An interesting next step would be to compare at high resolution how this morphology changes with the engagement of NKp30 receptor and if it correlates to our data on degranulation. Together with the other intriguing cell-DAAM-P interactions observed, this lays the foundation for future imaging studies and better understanding of IS formation and function.

4.7. NKG2D and NKp46 could also play a role in IS formation and degranulation

Our results showed that both NKG2D and NKp46 receptors had at least a ten times lower surface expression on KHYG-1 cells (**Figure 4**; **Figure S1**). Due to that, and to time limitations, they were not included in our assays. However, these receptors could also play a role in IS formation. We can speculate that they would promote degranulation and complex formation in a manner similar to NKp30, as they have been shown to activate NK-cell mediated killing (Wilton et al., 2019; Zamai et al., 2020). Future studies could consider testing their effect on IS formation with DAAM-Ps and degranulation with and without LFA-1 co-stimulation, as well as the interplay between these receptors, to further test that theory and improve our understanding of NK cell activity.

5. References

Allende-Vega, N., Marco Brualla, J., Falvo, P., Alexia, C., Constantinides, M., de Maudave, A. F., Coenon, L., Gitenay, D., Mitola, G., Massa, P., Orecchioni, S., Bertolini, F., Marzo, I., Anel, A., & Villalba, M. (2022). Metformin sensitizes leukemic cells to cytotoxic lymphocytes by increasing expression of intercellular adhesion molecule-1 (ICAM-1). *Scientific Reports*, *12*(1), 1341. https://doi.org/10.1038/s41598-022-05470-x

Ambrose, A. R., Hazime, K. S., Worboys, J. D., Niembro-Vivanco, O., & Davis, D. M. (2020). Synaptic secretion from human natural killer cells is diverse and includes supramolecular attack particles. *Proceedings of the National Academy of Sciences*, *117*(38), 23717–23720. https://doi.org/10.1073/pnas.2010274117

Barber, D. F., Faure, M., & Long, E. O. (2004). LFA-1 Contributes an Early Signal for NK Cell Cytotoxicity. *The Journal of Immunology*, *173*(6), 3653–3659. https://doi.org/10.4049/jimmunol.173.6.3653

Becker, P. S. A., Suck, G., Nowakowska, P., Ullrich, E., Seifried, E., Bader, P., Tonn, T., & Seidl, C. (2016). Selection and expansion of natural killer cells for NK cell-based immunotherapy. *Cancer Immunology, Immunotherapy*, *65*(4), 477–484. https://doi.org/10.1007/s00262-016-1792-y

Bio-Rad Laboratories. (2016). *'Proteus Protein A Antibody Purification Handbook'*.

Brandt, C. S., Baratin, M., Yi, E. C., Kennedy, J., Gao, Z., Fox, B., Haldeman, B., Ostrander, C. D., Kaifu, T., Chabannon, C., Moretta, A., West, R., Xu, W., Vivier, E., & Levin, S. D. (2009). The B7 family member B7-H6 is a tumor cell ligand for the activating natural killer cell receptor NKp30 in humans. *Journal of Experimental Medicine*, *206*(7), 1495–1503. https://doi.org/10.1084/jem.20090681

Butler, S. E., Brog, R. A., Chang, C. H., Sentman, C. L., Huang, Y. H., & Ackerman, M. E. (2022). Engineering a natural ligand-based CAR: directed evolution of the stress-receptor NKp30. *Cancer Immunology, Immunotherapy*, *71*(1), 165–176. https://doi.org/10.1007/s00262-021-02971-y

Cao, G., Wang, J., Zheng, X., Wei, H., Tian, Z., & Sun, R. (2015). Tumor Therapeutics Work as Stress Inducers to Enhance Tumor Sensitivity to Natural Killer (NK) Cell Cytolysis by Up-regulating NKp30 Ligand B7-H6. *Journal of Biological Chemistry*, *290*(50), 29964–29973. https://doi.org/10.1074/jbc.M115.674010

Capuano, C., Pighi, C., Battella, S., De Federicis, D., Galandrini, R., & Palmieri, G. (2021). Harnessing CD16-Mediated NK Cell Functions to Enhance Therapeutic Efficacy of Tumor-Targeting mAbs. *Cancers*, *13*(10), 2500. https://doi.org/10.3390/cancers13102500

Carisey, A. F., Mace, E. M., Saeed, M. B., Davis, D. M., & Orange, J. S. (2018). Nanoscale Dynamism of Actin Enables Secretory Function in Cytolytic Cells. *Current Biology*, *28*(4), 489-502.e9. https://doi.org/10.1016/j.cub.2017.12.044

Chen, Y., Lu, D., Churov, A., & Fu, R. (2020). Research Progress on NK Cell Receptors and Their Signaling Pathways. *Mediators of Inflammation*, *2020*, 1–14. https://doi.org/10.1155/2020/6437057

Correia, M. P., Stojanovic, A., Bauer, K., Juraeva, D., Tykocinski, L.-O., Lorenz, H.-M., Brors, B., & Cerwenka, A. (2018). Distinct human circulating NKp30 $^{+}$ FcεRIγ $^{+}$ CD8 $^{+}$ T cell population exhibiting high natural killer-like antitumor potential. *Proceedings of the National Academy of Sciences*, *115*(26). https://doi.org/10.1073/pnas.1720564115

Cross, S. E., Jin, Y.-S., Rao, J., & Gimzewski, J. K. (2007). Nanomechanical analysis of cells from cancer patients. *Nature Nanotechnology*, *2*(12), 780–783. https://doi.org/10.1038/nnano.2007.388

Duan, S., & Liu, S. (2022). Targeting NK Cells for HIV-1 Treatment and Reservoir Clearance. *Frontiers in Immunology*, *13*. https://doi.org/10.3389/fimmu.2022.842746

Freud, A. G., Mundy-Bosse, B. L., Yu, J., & Caligiuri, M. A. (2017). The Broad Spectrum of Human Natural Killer Cell Diversity. *Immunity*, *47*(5), 820–833. https://doi.org/10.1016/j.immuni.2017.10.008

Friedman, D., Simmonds, P., Hale, A., Bere, L., Hodson, N. W., White, M. R. H., & Davis, D. M. (2021). Natural killer cell immune synapse formation and cytotoxicity are controlled by tension of the target interface. *Journal of Cell Science*, *134*(7). https://doi.org/10.1242/jcs.258570

Guo, R., Chai, O., Hsien-I, C., Hospital, M., Li, C., Xu, Y., Guo, X., Liu, X., & Xu, Y. (2023). *B7-H6 promotes the killing activity of NK cells against cervical cancer through the downstream ERK pathway of NKp30*. https://doi.org/10.21203/rs.3.rs-3165739/v1

Gupta, M., Sarangi, B. R., Deschamps, J., Nematbakhsh, Y., Callan-Jones, A., Margadant, F., Mège, R.-M., Lim, C. T., Voituriez, R., & Ladoux, B. (2015). Adaptive rheology and ordering of cell cytoskeleton govern matrix rigidity sensing. *Nature Communications*, *6*(1), 7525. https://doi.org/10.1038/ncomms8525

Gutierrez-Silerio, G. Y., Bueno-Topete, M. R., Vega-Magaña, A. N., Bastidas-Ramirez, B. E., Gutierrez-Franco, J., Escarra-Senmarti, M., Pedraza-Brindis, E. J., Peña-Rodriguez, M., Ramos-Marquez, M. E., Delgado-Rizo, V., Banu, N., Alejandre-Gonzalez, A. G., Fafutis-Morris, M., Haramati, J., & del Toro-Arreola, S. (2023). Non-fitness status of peripheral <scp>NK</scp> cells defined by decreased <scp>NKp30</scp> and perforin, and increased soluble <scp>B7H6</scp> , in cervical cancer patients. *Immunology*, *168*(3), 538–553. https://doi.org/10.1111/imm.13593

Hjelm, H., Hjelm, K., & Sjöquist, J. (1972). Protein a from *Staphylococcus aureus* . Its isolation by affinity chromatography and its use as an immunosorbent for isolation of immunoglobulins. *FEBS Letters*, *28*(1), 73–76. https://doi.org/10.1016/0014-5793(72)80680-X

Hober, S., Nord, K., & Linhult, M. (2007). Protein A chromatography for antibody purification. *Journal of Chromatography B*, *848*(1), 40–47. https://doi.org/10.1016/J.JCHROMB.2006.09.030

Hui, K. L., Balagopalan, L., Samelson, L. E., & Upadhyaya, A. (2015). Cytoskeletal forces during signaling activation in Jurkat T-cells. *Molecular Biology of the Cell*, *26*(4), 685–695. https://doi.org/10.1091/mbc.E14-03-0830

Huse, M. (2017). Mechanical forces in the immune system. In *Nature Reviews Immunology* (Vol. 17, Issue 11, pp. 679–690). Nature Publishing Group. https://doi.org/10.1038/nri.2017.74

Hynes, R. O. (1992). Integrins: Versatility, modulation, and signaling in cell adhesion. *Cell*, *69*(1), 11–25. https://doi.org/10.1016/0092-8674(92)90115-S

Imai, K., Matsuyama, S., Miyake, S., Suga, K., & Nakachi, K. (2000). Natural cytotoxic activity of peripheral-blood lymphocytes and cancer incidence: an 11-year follow-up study of a general population. *The Lancet*, *356*(9244), 1795–1799. https://doi.org/10.1016/S0140-6736(00)03231-1

Jesus, M. de, Settle, A. H., Vorselen, D., Gaetjens, T. K., Galiano, M., Wong, Y. Y., Fu, T.-M., Santosa, E., Winer, B. Y., Tamzalit, F., Wang, M. S., Bao, Z., Sun, J. C., Shah, P., Theriot, J. A., Abel, S. M., & Huse, M. (2023). Topographical analysis of immune cell interactions reveals a biomechanical signature for immune cytolysis. *BioRxiv*, 2023.04.16.537078. https://doi.org/10.1101/2023.04.16.537078

Kim, C., Ye, F., & Ginsberg, M. H. (2011). Regulation of Integrin Activation. *Annual Review of Cell and Developmental Biology*, *27*(1), 321–345. https://doi.org/10.1146/annurev-cellbio-100109-104104

Kinashi, T. (2005). Intracellular signalling controlling integrin activation in lymphocytes. *Nature Reviews Immunology*, *5*(7), 546–559. https://doi.org/10.1038/nri1646

Klausz, K., Pekar, L., Boje, A. S., Gehlert, C. L., Krohn, S., Gupta, T., Xiao, Y., Krah, S., Zaynagetdinov, R., Lipinski, B., Toleikis, L., Poetzsch, S., Rabinovich, B., Peipp, M., & Zielonka, S. (2022). Multifunctional NK Cell–Engaging Antibodies Targeting EGFR and NKp30 Elicit Efficient Tumor

Cell Killing and Proinflammatory Cytokine Release. *The Journal of Immunology*, *209*(9), 1724–1735. https://doi.org/10.4049/jimmunol.2100970

Lanier, L. L. (2005). NK CELL RECOGNITION. *Annual Review of Immunology*, *23*(1), 225–274. https://doi.org/10.1146/annurev.immunol.23.021704.115526

Legate, K. R., Wickström, S. A., & Fässler, R. (2009). Genetic and cell biological analysis of integrin outside-in signaling. *Genes & Development*, *23*(4), 397–418. https://doi.org/10.1101/gad.1758709

Long, E. O., Sik Kim, H., Liu, D., Peterson, M. E., & Rajagopalan, S. (2013). Controlling Natural Killer Cell Responses: Integration of Signals for Activation and Inhibition. *Annual Review of Immunology*, *31*(1), 227–258. https://doi.org/10.1146/annurev-immunol-020711-075005

Lu, L., Ikizawa, K., Hu, D., Werneck, M. B. F., Wucherpfennig, K. W., & Cantor, H. (2007). Regulation of Activated CD4+ T Cells by NK Cells via the Qa-1–NKG2A Inhibitory Pathway. *Immunity*, *26*(5), 593–604. https://doi.org/10.1016/j.immuni.2007.03.017

Lv, J., Liu, Y., Cheng, F., Li, J., Zhou, Y., Zhang, T., Zhou, N., Li, C., Wang, Z., Ma, L., Liu, M., Zhu, Q., Liu, X., Tang, K., Ma, J., Zhang, H., Xie, J., Fang, Y., Zhang, H., … Huang, B. (2021). Cell softness regulates tumorigenicity and stemness of cancer cells. *The EMBO Journal*, *40*(2). https://doi.org/10.15252/embj.2020106123

Mandelboim, O., Lieberman, N., Lev, M., Paul, L., Arnon, T. I., Bushkin, Y., Davis, D. M., Strominger, J. L., Yewdell, J. W., & Porgador, A. (2001). Recognition of haemagglutinins on virus-infected cells by NKp46 activates lysis by human NK cells. *Nature*, *409*(6823), 1055–1060. https://doi.org/10.1038/35059110

Matalon, O., Ben-Shmuel, A., Kivelevitz, J., Sabag, B., Fried, S., Joseph, N., Noy, E., Biber, G., & Barda-Saad, M. (2018). Actin retrograde flow controls natural killer cell response by regulating the conformation state of <scp>SHP</scp> -1. *The EMBO Journal*, *37*(5). https://doi.org/10.15252/embj.201696264

Meza Guzman, L. G., Keating, N., & Nicholson, S. E. (2020). Natural Killer Cells: Tumor Surveillance and Signaling. *Cancers*, *12*(4), 952. https://doi.org/10.3390/cancers12040952

New England Biolabs. (2024). *Affinity of Protein A/G for IgG Types from Different Species*. https://www.neb.com/en/tools-and-resources/selection-charts/affinity-of-protein-ag-for-igg-types-from-different-species

Niek Frijlink. (2023). *The Forces of a Natural Killer Cell*. Wageningen University & Research.

Orange, J. S. (2006). Human natural killer cell deficiencies. *Current Opinion in Allergy and Clinical Immunology*, *6*(6), 399–409. https://doi.org/10.1097/ACI.0b013e3280106b65

Orange, J. S. (2008). Formation and function of the lytic NK-cell immunological synapse. In *Nature Reviews Immunology* (Vol. 8, Issue 9, pp. 713–725). https://doi.org/10.1038/nri2381

Orange, J. S., Harris, K. E., Andzelm, M. M., Valter, M. M., Geha, R. S., & Strominger, J. L. (2003). The mature activating natural killer cell immunologic synapse is formed in distinct stages. *Proceedings of the National Academy of Sciences*, *100*(24), 14151–14156. https://doi.org/10.1073/pnas.1835830100

Piccioli, D., Sbrana, S., Melandri, E., & Valiante, N. M. (2002). Contact-dependent Stimulation and Inhibition of Dendritic Cells by Natural Killer Cells. *The Journal of Experimental Medicine*, *195*(3), 335–341. https://doi.org/10.1084/jem.20010934

Pinheiro, P. F., Justino, G. C., & Marques, M. M. (2020). NKp30 - A prospective target for new cancer immunotherapy strategies. *British Journal of Pharmacology*, *177*(20), 4563–4580. https://doi.org/10.1111/bph.15222

Ponjavic, A., McColl, J., Carr, A. R., Santos, A. M., Kulenkampff, K., Lippert, A., Davis, S. J., Klenerman, D., & Lee, S. F. (2018). Single-Molecule Light-Sheet Imaging of Suspended T Cells. *Biophysical Journal*, *114*(9), 2200–2211. https://doi.org/10.1016/j.bpj.2018.02.044

Prager, I., & Watzl, C. (2019). Mechanisms of natural killer cell-mediated cellular cytotoxicity. *Journal of Leukocyte Biology*, *105*(6), 1319–1329. https://doi.org/10.1002/JLB.MR0718-269R

Rabinovich, B. A., Li, J., Shannon, J., Hurren, R., Chalupny, J., Cosman, D., & Miller, R. G. (2003). Activated, But Not Resting, T Cells Can Be Recognized and Killed by Syngeneic NK Cells. *The Journal of Immunology*, *170*(7), 3572–3576. https://doi.org/10.4049/jimmunol.170.7.3572

Ritter, A. T., Asano, Y., Stinchcombe, J. C., Dieckmann, N. M. G., Chen, B.-C., Gawden-Bone, C., van Engelenburg, S., Legant, W., Gao, L., Davidson, M. W., Betzig, E., Lippincott-Schwartz, J., & Griffiths, G. M. (2015). Actin Depletion Initiates Events Leading to Granule Secretion at the Immunological Synapse. *Immunity*, *42*(5), 864–876. https://doi.org/10.1016/j.immuni.2015.04.013

Schmiedel, D., & Mandelboim, O. (2018). NKG2D Ligands–Critical Targets for Cancer Immune Escape and Therapy. *Frontiers in Immunology*, *9*. https://doi.org/10.3389/fimmu.2018.02040

Sen Santara, S., Lee, D.-J., Crespo, Â., Hu, J. J., Walker, C., Ma, X., Zhang, Y., Chowdhury, S., Meza-Sosa, K. F., Lewandrowski, M., Zhang, H., Rowe, M., McClelland, A., Wu, H., Junqueira, C., & Lieberman, J. (2023). The NK cell receptor NKp46 recognizes ecto-calreticulin on ER-stressed cells. *Nature*, *616*(7956), 348–356. https://doi.org/10.1038/s41586-023-05912-0

Shabrish, S., Gupta, M., & Madkaikar, M. (2016). A Modified NK Cell Degranulation Assay Applicable for Routine Evaluation of NK Cell Function. *Journal of Immunology Research*, *2016*, 1–6. https://doi.org/10.1155/2016/3769590

Shan, J., Jing, W., Ping, Y., Shen, C., Han, D., Liu, F., Liu, Y., Li, C., & Zhang, Y. (2024). LFA-1 regulated by IL-2/STAT5 pathway boosts antitumor function of intratumoral CD8 $^{+}$ T cells for improving anti-PD-1 antibody therapy. *OncoImmunology*, *13*(1). https://doi.org/10.1080/2162402X.2023.2293511

Shi, H., & Shao, B. (2023). LFA-1 Activation in T-Cell Migration and Immunological Synapse Formation. *Cells*, *12*(8), 1136. https://doi.org/10.3390/cells12081136

Siemaszko, J., Marzec-przyszlak, A., & Bogunia-kubik, K. (2021). Nkg2d natural killer cell receptor—a short description and potential clinical applications. In *Cells* (Vol. 10, Issue 6). MDPI. https://doi.org/10.3390/cells10061420

Taylor, C. R., Shi, S.-R., Barr, N. J., & Wu, N. (2006). Techniques of Immunohistochemistry: Principles, Pitfalls and Standardization. In *Diagnostic Immunohistochemistry* (pp. 1–42). Elsevier. https://doi.org/10.1016/B978-0-443-06652-8.50007-7

Trinchieri, G. (1989). *Biology of Natural Killer Cells* (pp. 187–376). https://doi.org/10.1016/S0065-2776(08)60664-1

Urlaub, D., Höfer, K., Müller, M.-L., & Watzl, C. (2017). LFA-1 Activation in NK Cells and Their Subsets: Influence of Receptors, Maturation, and Cytokine Stimulation. *The Journal of Immunology*, *198*(5), 1944–1951. https://doi.org/10.4049/jimmunol.1601004

Vorselen, D., Wang, Y., de Jesus, M. M., Shah, P. K., Footer, M. J., Huse, M., Cai, W., & Theriot, J. A. (2020). Microparticle traction force microscopy reveals subcellular force exertion patterns in immune cell–target interactions. *Nature Communications*, *11*(1). https://doi.org/10.1038/s41467-019-13804-z

Voskoboinik, I., Smyth, M. J., & Trapani, J. A. (2006). Perforin-mediated target-cell death and immune homeostasis. *Nature Reviews Immunology*, *6*(12), 940–952. https://doi.org/10.1038/nri1983

Walling, B. L., & Kim, M. (2018). LFA-1 in T Cell Migration and Differentiation. *Frontiers in Immunology*, *9*. https://doi.org/10.3389/fimmu.2018.00952

Wang, H., Zheng, X., Wei, H., Tian, Z., & Sun, R. (2012). Important Role for NKp30 in Synapse Formation and Activation of NK Cells. *Immunological Investigations*, *41*(4), 367–381. https://doi.org/10.3109/08820139.2011.632799

Wang, M. S., Hu, Y., Sanchez, E. E., Xie, X., Roy, N. H., de Jesus, M., Winer, B. Y., Zale, E. A., Jin, W., Sachar, C., Lee, J. H., Hong, Y., Kim, M., Kam, L. C., Salaita, K., & Huse, M. (2022). Mechanically active integrins target lytic secretion at the immune synapse to facilitate cellular cytotoxicity. *Nature Communications*, *13*(1), 3222. https://doi.org/10.1038/s41467-022-30809-3

Wilton, K. M., Overlee, B. L., & Billadeau, D. D. (2019). NKG2D/DAP10 Signaling recruits EVL to the cytotoxic synapse to generate F-actin and promote NK cell cytotoxicity. *Journal of Cell Science*. https://doi.org/10.1242/jcs.230508

Wong, D. C. P., & Ding, J. L. (2023). The mechanobiology of NK cells- 'Forcing NK to Sense' target cells. *Biochimica et Biophysica Acta (BBA) - Reviews on Cancer*, *1878*(2), 188860. https://doi.org/10.1016/j.bbcan.2023.188860

Xie, G., Dong, H., Liang, Y., Ham, J. D., Rizwan, R., & Chen, J. (2020). CAR-NK cells: A promising cellular immunotherapy for cancer. *EBioMedicine*, *59*, 102975. https://doi.org/10.1016/j.ebiom.2020.102975

Zamai, L., Del Zotto, G., Buccella, F., Gabrielli, S., Canonico, B., Artico, M., Ortolani, C., & Papa, S. (2020). Understanding the Synergy of NKp46 and Co-Activating Signals in Various NK Cell Subpopulations: Paving the Way for More Successful NK-Cell-Based Immunotherapy. *Cells*, *9*(3). https://doi.org/10.3390/cells9030753

Zarrineh, M., Mashhadi, I. S., Farhadpour, M., & Ghassempour, A. (2020). Mechanism of antibodies purification by protein A. *Analytical Biochemistry*, *609*, 113909. https://doi.org/10.1016/j.ab.2020.113909

Zhang, T., Wu, M.-R., & Sentman, C. L. (2012). An NKp30-Based Chimeric Antigen Receptor Promotes T Cell Effector Functions and Antitumor Efficacy In Vivo. *The Journal of Immunology*, *189*(5), 2290–2299. https://doi.org/10.4049/jimmunol.1103495

Zuo, W., & Zhao, X. (2021). Natural killer cells play an important role in virus infection control: Antiviral mechanism, subset expansion and clinical application. *Clinical Immunology*, *227*, 108727. https://doi.org/10.1016/j.clim.2021.108727

Appendix I – Supplemental figures

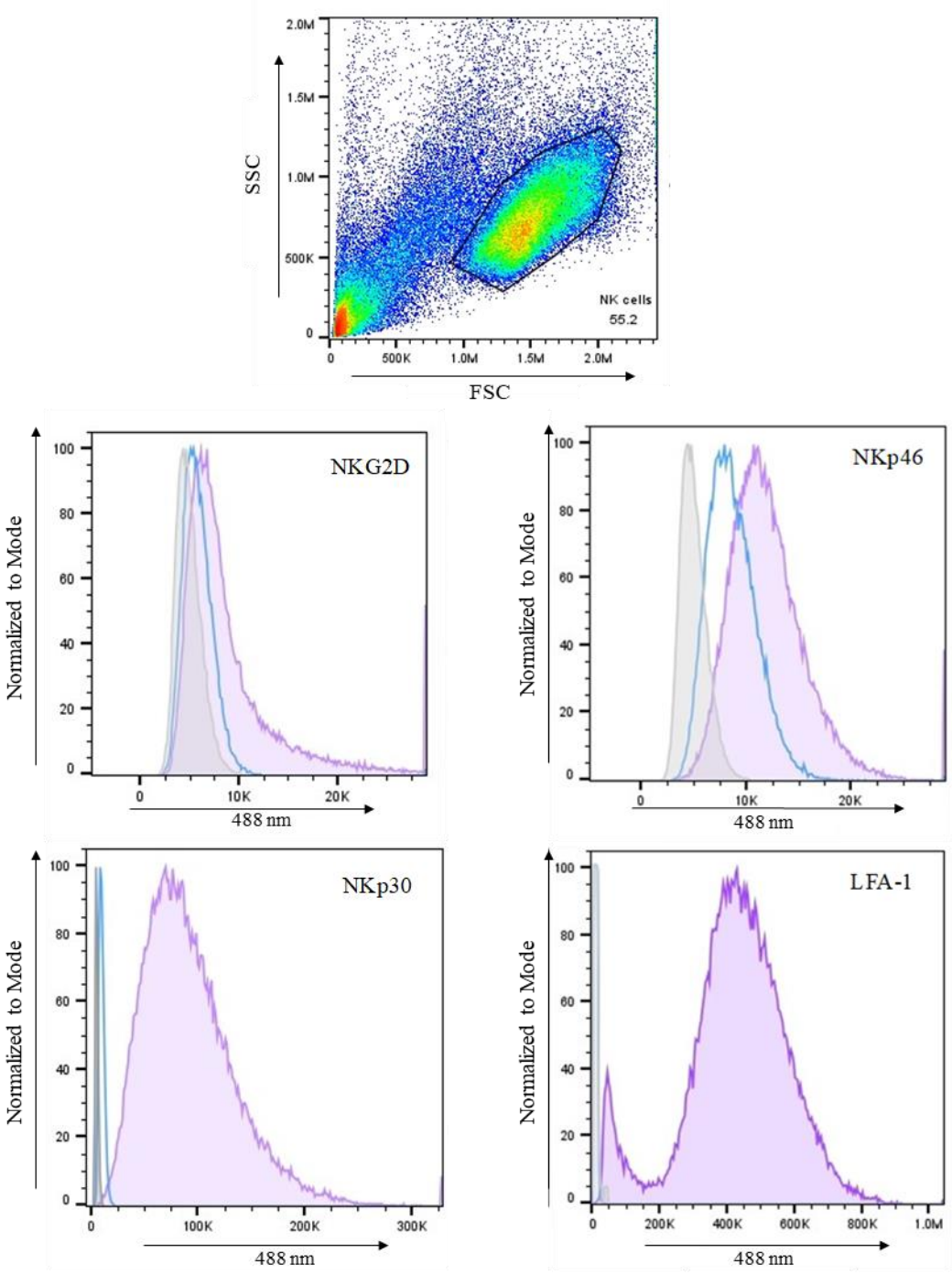

Figure S1. Staining surface expression of NKG2D, NKp30, NKp46 and LFA-1 on KHYG-1 cells. Cells were stained using receptor specific primary antibodies/recombinant proteins and secondary antibodies conjugated with AlexaFluor 488. Dot plot shows the gating strategy for selecting NK cell population. Histograms show the expression of corresponding receptors when compared to background and secondary antibody control. Gray – background signal, blue line – secondary antibody control, purple – receptor staining.

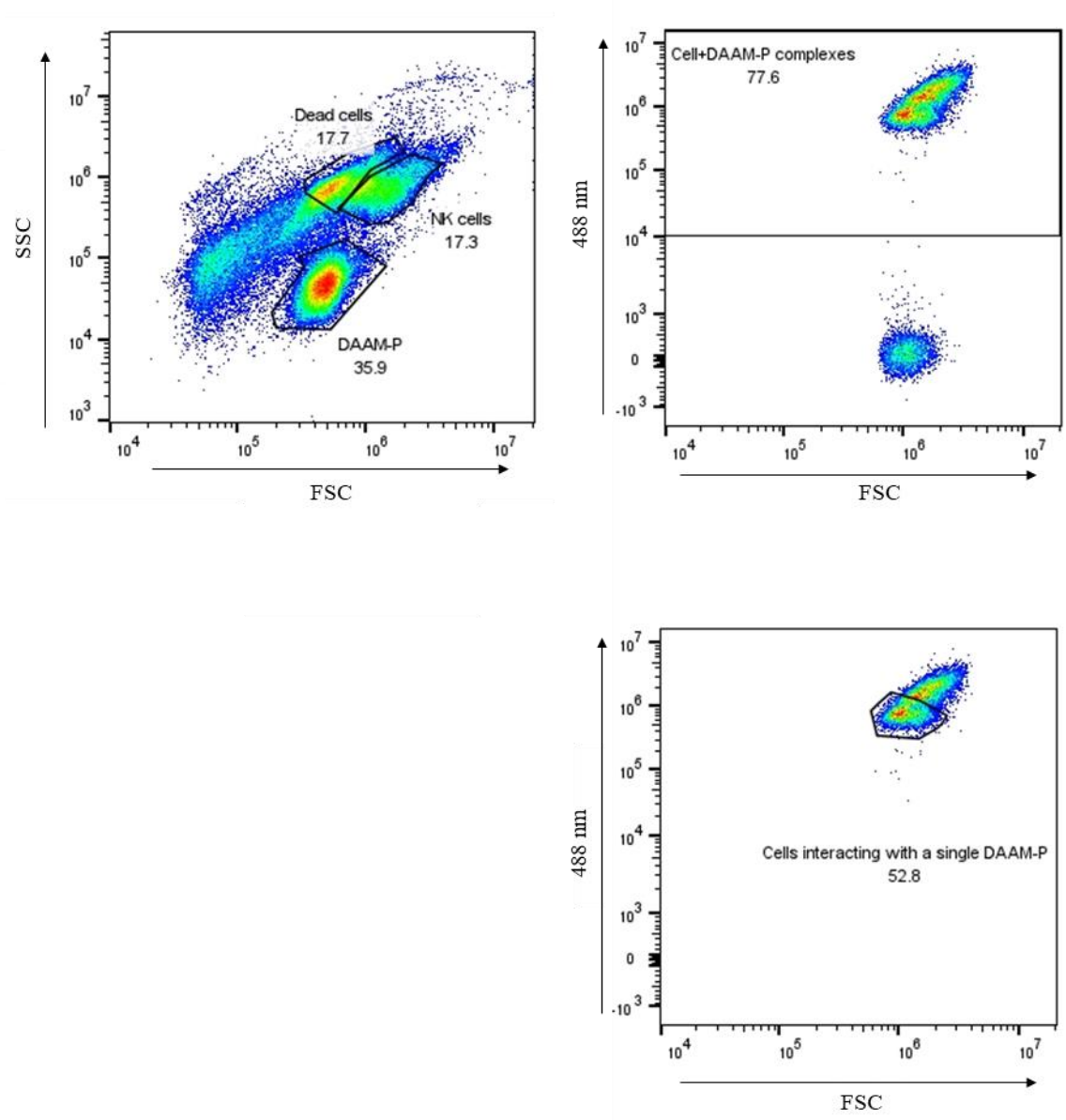

Figure S2. Gating strategy for analysing immune complex formation. KHYG-1 cells were incubated for 15 min with DAAM-P functionalized with FITC-cadaverine, protein A and 2,5 µg/ml anti-LFA-1 antibodies. NK cells were selected based on forward and side scatter. Complex formation was analysed by gating the cells that emitted fluorescence corresponding to FITC. To check for single DAAM-P/cell interactions, a gate was created based on area and width of DAAM-P forward scatter and adjusted to fit the NK cell plot. Top left, all events. Top right, NK cells. Bottom right, NK cell/DAAM-P complexes.

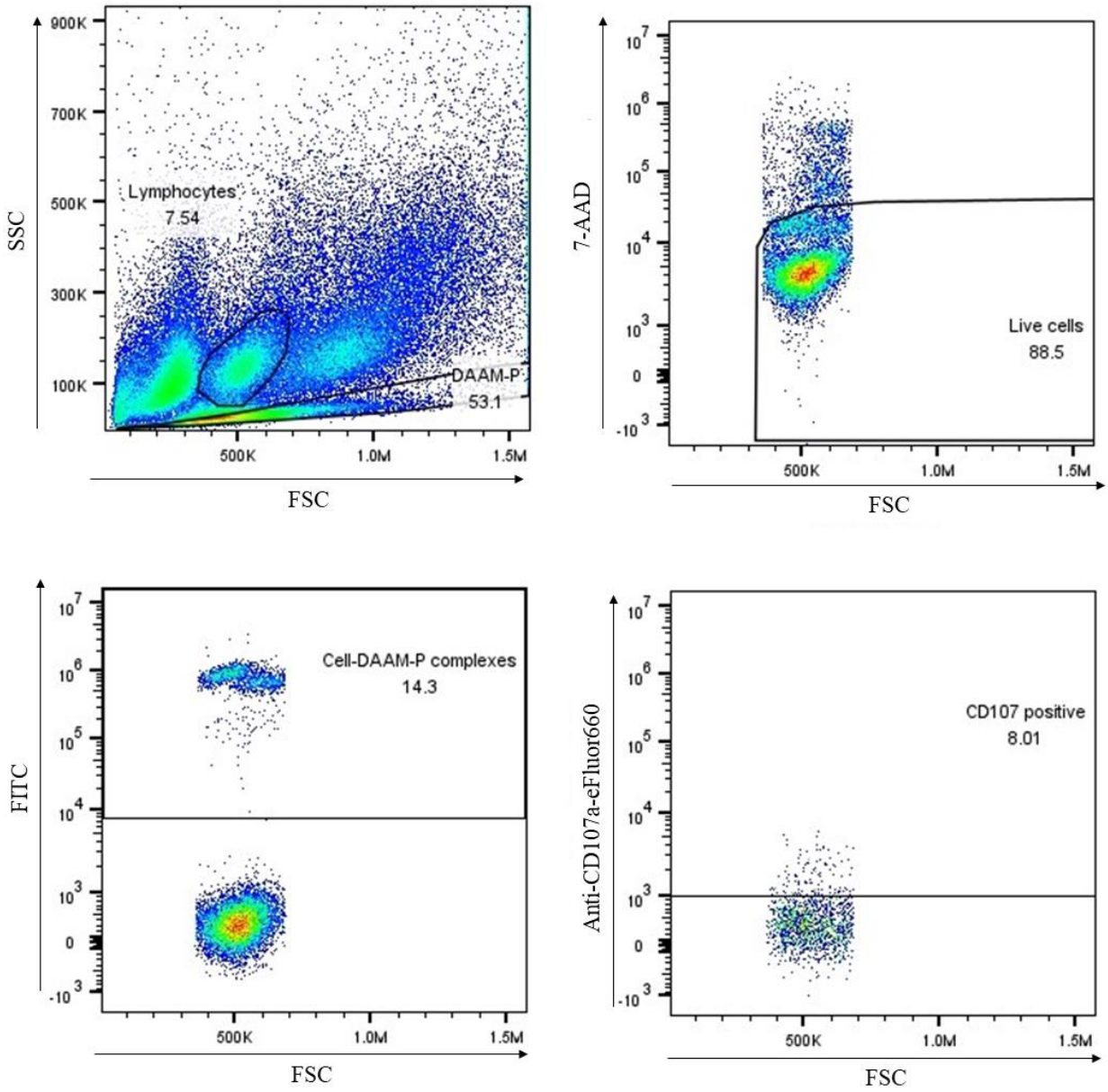

Figure S3. Gating strategy for analysing lymphocyte activation in PBMC activation assay. PBMCs were incubated with DAAM-Ps functionalized with protein A, FITC-cadaverine and 2,5 µg/ml anti-LFA-1 antibodies for 30 min. Lymphocytes were selected based on forward and side scatter. Live lymphocytes were selected based on the signal from 7-AAD marker. Complex formation was analysed based on FITC signal and cells in the complexes were then checked for CD107a expression. Top left: all cells. Top right: lymphocytes. Bottom left: Live lymphocytes. Bottom right: live lymphocyte/DAAM-P complexes.

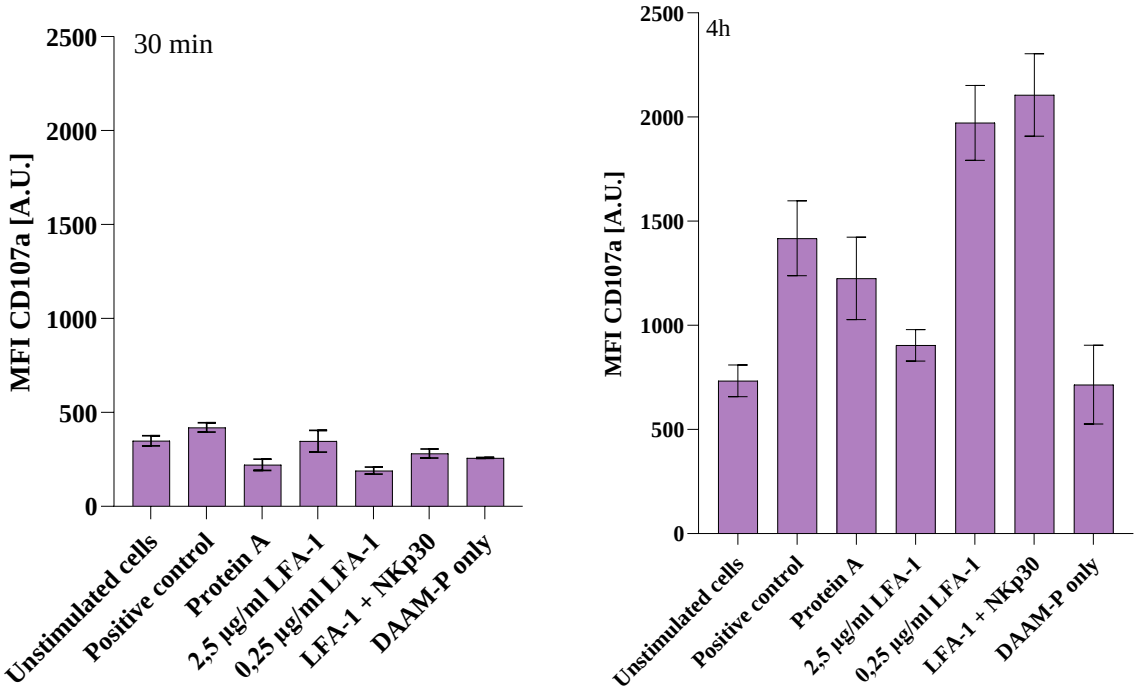

Figure S4. Degranulation of all live lymphocytes in PBMC activation assay. PBMCs were incubated with DAAM-Ps functionalized with FITC-cadaverine, protein A and anti-LFA-1 antibodies at different concentrations or with anti-NKp30 antibodies at 25 µg/ml and anti-LFA-1 at 0,25 µg/ml for 30 min and 4h. Protein A DAAM-Ps without antibodies were used as control. PBMCs with PMA and ionomycin were used as positive control. Live lymphocytes were selected based on FSC, SSC and 7-AAD marker. Degranulation marker CD107a was detected using rat anti-CD107a-eFluor660 antibodies in all samples. As these samples included all live lymphocytes background CD107a signal from DAAM-Ps is shown on the graph but was not subtracted, since not all of the cells are engaged in cell/DAAM-P complexes. Error bars represent standard error of the mean (SEM) of the CD107a signal in a single sample.

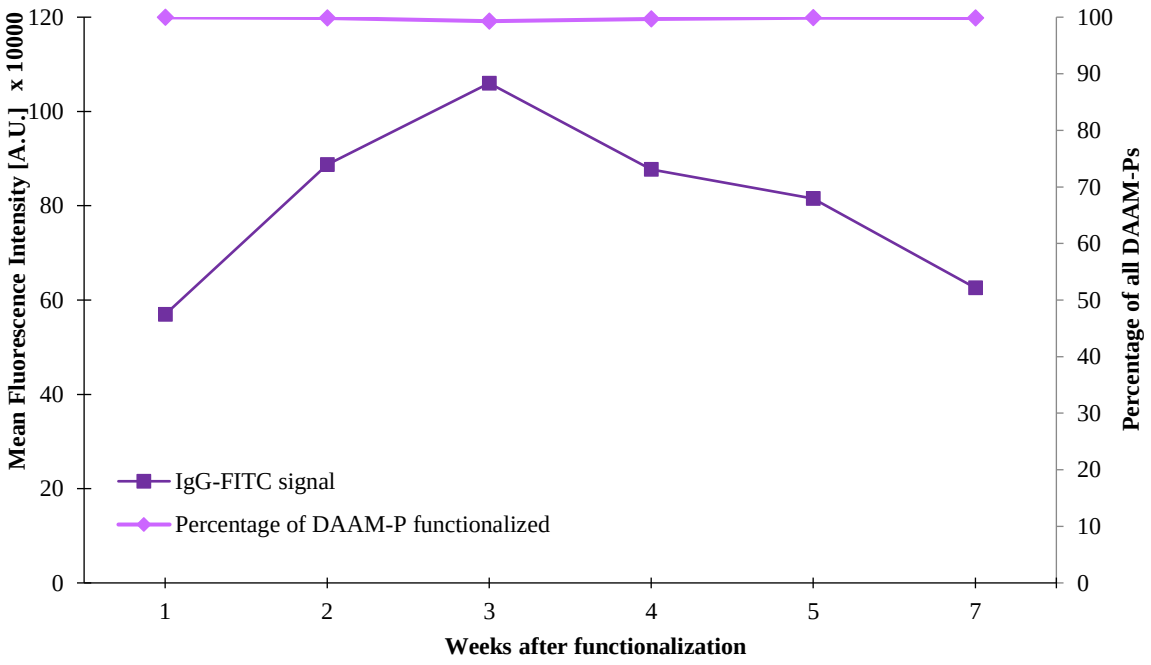

Figure S5. Stability of protein A DAAM-Ps over time. DAAM-Ps were functionalized with protein A and TMR- cadaverine and then coupled with rabbit IgG-FITC antibodies every week and measured on a flow cytometer. Stability was assessed based on the FITC signal from antibodies bound to protein A on DAAM-Ps. There was no noticeable change in stability over the tested time period (7 weeks), differences from fluorescence intensity were due to the difficulty to pipet the exact same DAAM-P number in each measurement.

Appendix II – Protocols

Protocol 1 – Staining surface receptors on KHYG-1 cells

Materials:

- KHYG-1 cells
- FACS buffer (10 mg/ml BSA, 0,5mM EDTA in PBS pH 7,4)
- Antibodies and fluorophores:
    - Recombinant human chimera protein MICA-Fc
    - Anti-NKp46 rabbit, anti-NKp30 mouse, anti-LFA-1 rabbit antibodies
    - AlexaFluor 488 goat anti-human 1:1000
    - AlexaFluor 488 goat anti-rabbit 1:1000
    - AlexaFluor 488 goat anti-mouse 1:1000

Plate setup primary antibodies and ligands (NS – non-stained):

	1	2	3	4	5	6	7	8	9	10
A	MICA-Fc 0,1ug/ml	MICA-Fc 1ug/ml	MICA-Fc 10ug/ml	aNKp46 10 ug/ml	aNKp30 1ug/ml	aLFA-1 5ug/ml	NS	NS	NS	NS
B	MICA-Fc 0,1ug/ml	MICA-Fc 1ug/ml	MICA-Fc 10ug/ml	aNKp46 10 ug/ml	aNKp30 1ug/ml	aLFA-1 5ug/ml	NS	NS	NS	NS
C	MICA-Fc 0,1ug/ml	MICA-Fc 1ug/ml	MICA-Fc 10ug/ml	aNKp46 10 ug/ml	aNKp30 1ug/ml	aLFA-1 5ug/ml	NS	NS	NS	NS

Plate setup secondary antibodies and markers:

	1	2	3	4	5	6	7	8	9	10
A	AF488 anti-human	AF488 anti-human	AF488 anti-human	AF488 goat anti-rabbit	AF488 goat anti-mouse	AF488 goat anti-rabbit	AF488 anti-human	AF488 goat anti-rabbit	AF488 goat anti-mouse	NS
B	AF488 anti-human	AF488 anti-human	AF488 anti-human	AF488 goat anti-rabbit	AF488 goat anti-mouse	AF488 goat anti-rabbit	AF488 anti-human	AF488 goat anti-rabbit	AF488 goat anti-mouse	NS
C	AF488 anti-human	AF488 anti-human	AF488 anti-human	AF488 goat anti-rabbit	AF488 goat anti-mouse	AF488 goat anti-rabbit	AF488 anti-human	AF488 goat anti-rabbit	AF488 goat anti-mouse	NS

Before experiment: prepare calculations for ab mix

Protein	Final volume [µl]	Antibody stock [µg/ml]	Antibody concentration [µg/ml]	Antibody volume [µl]	FACS buffer volume [µl]
MICA-Fc	50	1470	50	1,7	48,3
MICA-Fc	200	50	10	40,0	160,0
MICA-Fc	200	10	1	20,0	180,0
MICA-Fc	200	1	0,1	20,0	180,0

Antibody	Final volume [µl]	Antibody stock [µl [µg/ml]	Antibody concentration [µg/ml]	Antibody volume [µl]	FACS buffer volume [µl]
aNKp46	160	500	10	3,2	156,8
aNKp30	20	500	50	2,0	18,0
aNKp30	160	50	1	3,2	156,8
aLFA-1	200	1000	5	1,0	199,0

1:1000 dilutions of secondary AF488 anti human antibodies (12 wells):

- Dilute 1:100, 2µl in 200µl
- Dilute 1:1000 by adding 100µl of 1:100 in 1000µl

1:1000 dilutions of secondary AF488 anti rabbit antibodies (9 wells):

- Dilute 1:100, 1µl in 100µl
- Dilute 1:1000 by adding 50ul of 1:100 in 500ul

1:1000 dilutions of secondary AF488 anti mouse antibodies (6 wells):

- Dilute 1:100, 1µl in 100µl
- Dilute 1:1000 by adding 50µl of 1:100 in 500µl

Protocol cells:

- Turn on flow cytometer
- Prepare antibody mixes
- Count cells (cells in 25 squares X dilution factor X 10^4= nr of cells/ ml) (3x10^6 cells needed for 30 wells)
- Spin 5 min 500g
- Resuspend in FACS buffer at 500 000 cells/ml (6ml total)
- Transfer to 96 well round bottom plate (200µl/well (100 000 cells)
- Place on ice
- Spin (2'400g), use tissue to remove all fluid and resuspend pellet using vortex
- Add 1st Ab in 50 µl volume (and 50 µl FACS buffer to cells that do not need antibody in this step), mix
- Incubate 20 min 4° or on ice
- Spin (2'400g), use tissue to remove all fluid and resuspend pellet using vortex
- add 2nd Ab in 50 µl volume, mix
- incubate 20 min 4° or on ice
- spin (2'400g), use tissue to remove all fluid and resuspend pellet using vortex
- Resuspend in 150µl FACS buffer
- FACS analysis

Update this info for your antibodies and add to your protocol so that you know in advance which laser your need to use

488	525/40 BP	B525-FITC	FITC, AF488, CFSE, Fluo-3

Protocol 2 – DAAM-P functionalization with protein A and carboxyl-reactive dyes

Required reagents:

- EDC: N-(3-Dimethylaminopropyl)-N′-ethylcarbodiimide hydrochloride (Sigma: E7750)
- NHS: N-Hydroxysuccimide (Thermo Fisher Scientific: 24500)
- MES sodium salt (Sigma: M5057)
- Ethanolamine (Sigma: 398136)
- tris(hydroxymethyl)aminomethane
- Tween (polysorbate) 20
- Sodium azide
- NaCl
- A dye with a primary amine[1]
- Protein/peptide of interest

Reagent setup:

Prepare the following solutions/buffers.

- 10% tween 20 (store for ~1 month, prepare new if it has visible precipitation or does not foam when shaken)
- PBS (pH 7.4)
- PBS + 0.1 % tween 20 (pH 7.4)[2]
- PBS + 0.1 % tween 20 (pH 8.0)
- 0.1x PBS (pH6) +0.2% tween 20
- 2x PBS (pH8.5)
- Activation buffer: 100 mM MES (sodium salt) pH 6.0 + 200mM NaCl (Store at 4C for max 6 months)
    - 15 mL stock .33 M NaMES (4C) + 5 mL 2 M NaCl + 30 mL mQ
- Blocking buffer: 300 mM Tris (pH 9.0) + 300 mM NaCl
- 10% w/v sodium azide

1. Dilute beads to 5% solids in activation buffer - for stiff 14,7um 5kPa: 250ul of beads+950ul of activation buffer; for soft 11,3um 1kPa (15%):400ul beads + 800ul buffer
2. Update stock concentrations here with the current volume
3. Prepare the protein solutions (copy A17:E24 from bead functionalization setup:

Coupling mix				
Beads - original volume (@5%)	Bead volume	C protein desired	C Protein stock	V protein stock
mL	mL	mg/mL	mg/mL	uL
1,2	0,6	10	20	600
1,2	0,96	10	50	240

4. Prepare the carboxyl-reactive dyes (copy A28:E35 from bead functionalization setup):

Fluorescence blocking mix				
Bead volume (mL)	Fluorophore	C fluor (mM)	C fluor stock (mM)	V fluorophore (uL)
1,2	FITC	0,2	40	6
1,2	FITC	0,2	40	6

5. Weigh out EDC/NHS for the activation mix and dissolve in activation buffer:

EDC	96	mg
NHS	48	mg

6. Wash the beads 2x in Activation buffer at 1000 g for 1 minute, mix rigorously in between

7. Resuspend the beads in Activation buffer
8. Mix in the order indicated and vortex after every step(see A5:D12 from bead functionalization setup):

beads (mL)	10% tween (uL)	EDC (mL)	NHS (mL)
0,72	12	0,24	0,24
0,72	12	0,24	0,24

9. Incubate while mixing at RT for 15 min.
10. Wash beads 3x with 0.1 X PBS (pH 6) + 0.2% tween 20 by spinning 1 min at 1000 g
11. Resuspend in 0.5 x original volume
12. Add 0.5 x original volume 2X PBS pH 8.5. Handle quickly, pipette up and down twice to mix and immediately add to the protein
13. Aliquot beads in the tube with protein. Incubate for 1h.
14. Aliquot the beads in the tubes with cadaverine. Incubate for 30 min
15. Meanwhile, make the blocking mix (see H39:N42 from bead functionalization setup):

Total Volume		final concentration	Concentration mix	Mix amounts:	Stock solutions.	
2,4		mM	mM	mL	mM	
	Tris (pH 9) + NaCl	100	300	1,2	300	
	ethanolamine	100	300	0,022	16560	(pure)

16. Add 0.5x the current volume blocking mix to each tube (see B40:B47 from bead functionalization setup)
17. Incubate for 30 min
18. Wash beads 4x in 1 mL PBS (pH 7.4), including 0.1% tween 20, spin 1min at 1000 g
19. For final wash, resuspend in the original volume of PBS (pH 7.4), including 0.1% tween 20
20. Store at 4°C with sodium azide, add 3 uL 10% azide per 1 mL (~5mM final concentration)

Protocol 3 – Coupling protein A DAAM-P with antibodies

1. Take desired volume of protein A functionalized DAAM-P.

Antibody	DAAM-P number	DAAM-P volume [µl]
Anti-LFA-1	10^6	100
Anti-LFA-1	10^6	100
Anti-LFA-1	10^6	100
Anti-LFA-1	10^6	100
Anti-LFA-1	10^6	100

2. Prepare antibody solutions in PBS (pH 9):

Antibody	Final volume [µl]	Antibody stock [µg/ml]	Antibody concentration [µg/ml]	Antibody volume [µl]	PBS volume [µl]
Anti-LFA-1	150	1000	25	3,8	146,3
Anti-LFA-1	150	25	8	48,0	102,0
Anti-LFA-1	150	8	2,5	46,9	103,1
Anti-LFA-1	150	2,5	0,8	48,0	102,0
Anti-LFA-1	150	0,8	0,25	46,9	103,1

3. Spin beads at 1000g for 1 min and remove liquid
4. Add 100 µl of antibody to each tube.
5. Incubate at RT while shaking for 1h.
6. Wash 2x in PBS (pH 9) with 0,1% Tween spin 1 min 1000g
7. Wash 1x in PBS (pH 9) spin 1 min 1000g
8. If stored for >1 day add 5 mM sodium azide (3 µl per 1 ml)

Protocol 4 - NK cell activation assay in PBMCs with degranulation marker CD107a

Materials:

- Human PBMCs
- PBMC cell medium (RPMI, 10% FBS, 0.1% penicillin/streptomycin
- 14 mL round bottom tubes with a lid
- Functionalized DAAM-P
- PBA (PBS & 0.5% BSA & EDTA & NaAz)
- 96 well NUNC FACS plate
- UltraComp eBeads Plus Compensation Beads
- Golgistop: 0.5 µL/sample 1:1000 dilution
- Anti-CD107-eFluor 660 stock 0,2 mg/ml: 2,5 µg/ml /sample
- PMA (0.5 µL/sample) and ionomycin (2.5 µL/sample)
- CD56-PE (1:25)
- Viability staining solution 7-Aminoactinomycin D (7-AAD) 5 230l per samples, add just before going to the FACS

Settings:

- (A1) Unstained beads
- (A2) eFluor660-stained beads
- (A3) CD56-stained beads
- (A4) PercP-Cy5.5-stained beads
- (A5) FITC stained DAAM-P
- (A6) Unstained PBMCs

Samples:

- 30min:
    - unstimulated,
    - DAAM-P control (protein A, no abs),
    - DAAM-P+2,5 ug/ml aLFA-1,
    - DAAM-P+0,25 ug/ml aLFA-1,
    - DAAM-P+25ug/ml aNKp30+0,25ug/ml aLFA-1,
    - DAAM-P only (no cells),
    - positive control PMA/ Ionomycin
    - cells only (for settings)
- 4h: :
    - unstimulated,
    - DAAM-P control (protein A, no abs),
    - DAAM-P+2,5 ug/ml aLFA-1,
    - DAAM-P+0,25 ug/ml aLFA-1,
    - DAAM-P+25ug/ml aNKp30+0,25ug/ml aLFA-1,
    - DAAM-P only (no cells),
    - positive control PMA/ionomycin

Protocol:

Functionalize DAAM-P the day before with antibodies, resuspend in medium:

- 10^6 DAAM-P per condition in 250ul medium (10^6 DAAM-P in total)

Prepare Golgistop/antibody mix:

- Golgistop: 0.5 µL/sample, CD107-eFluor660: 2,5 µg/ml /sample, stock 0,2mg/ml → 6,25 ul per sample
- 14 samples
- 0.5 µL x 15 + 6,25 µL x 15 = 101,25 µL (you lose some fluid with pipetting) --> take 6,75 µL for every sample

Thaw PBMCs:

- Preparations: switch on the water bath, clean flow, write tube, switch on centrifuge at 4 degrees, make sure that everything you need is ready. You want to do the thawing as fast as possible.
- Take cryovial out of liquid nitrogen storage and transfer to 37°C water bath

- Once only few ice crystals are visible, remove vial from bath and clean with isopropyl alcohol. Dry afterwards with a tissue to make sure that all isopropanol is gone
- Transfer cell suspension to 15 mL tube and add 13 mL of cold medium drip by drip while continuously shaking the tube
- Spin tube 1300 rpm for 5 min at 4°C
- Discard supernatant, resuspend pellet and add 15 mL medium
- Spin tube 1300 rpm for 5 min at 4°C
- Discard supernatant and resuspend cells in 6 mL medium

Stimulate cells:

- Add 20 µL cells and 20 µL Trypan Blue to Eppendorf tube
- Count cells (number of cells in 25 squares • dilution factor • 10^4 = number of cells / mL)
- Adjust concentration of cells to $2•10^6$ cells/mL
- Add 0.25 mL cell suspension (500 000 cells) per sample to a 14 ml round bottom tube with a lid
- Add 0.25 mL medium with corresponding DAAM-P to each tube that has to be stimulated
- Add 0.25 mL medium to each tube that does not have to be stimulated
- Add 6,75 µL of Golgistop/antibody mix to each sample
- Add 0.5 µL PMA and 2.5 µL ionomycin to each positive control sample
- Mix by tapping the rack in which tubes are placed
- Incubate all samples at 37°C while shaking.

After 30 min

- Take 30 min tubes out of incubator,
- Pipet through a 70 µm strainer cap (FACS tubes with blue cap) to remove large cell/DAAM-P clusters
- Place on ice and wash samples with cold PBA (3 mL/sample)
- Spin tubes 3 minutes 1300 rpm 4°C, discard supernatant, resuspend using vortex
- Resuspend in 200 µl FACSbuffer
- Store in the fridge until 4h samples are ready

After 3.5 hours, prepare beads in 96 well NUNC FACS plate: (you can also do this earlier and store the stained beads in the fridge as well)

- Add one droplet/well of UltraComp eBeads Plus Compensation Beads to 4 wells of FACS plate (A1-A4)
- Add 1 µL of each antibody individually to a well, quickly mix by gently tapping to plate
- Incubate in aluminum foil in fridge for 20 min
- Wash with PBA (200 µL/well)
- Spin plate 2 minutes 1300 rpm 4°C, use tissue to remove all fluid, resuspend using vortex

After 4 hours, prepare antibody mix and prepare flow cytometry analysis:

- Prepare antibody mix according to table below

	Antibody	Dilution	Final volume
Antibody mix	PBA CD56-PE (1:25)	720 µL 30 µL	750 µL

- Take 4h tubes out of incubator,
- Pipet through a 70 µm strainer cap (FACS tubes with blue cap) to remove large cell/DAAM-P clusters
- place on ice and wash samples with cold PBA (3 mL/sample)
- Spin tubes 3 minutes 1300 rpm 4°C, discard supernatant, resuspend using vortex
- Add 50 µL antibody mix to every sample
- Incubate 20 min on ice covered with aluminum foil
- Wash samples with PBA (3 mL/sample), keep on ice
- Spin tubes 5 minutes 1300 rpm 4°C, discard supernatant, resuspend using vortex
- Add 200 µL PBA and transfer to the prepared 96 well NUNC FACS plate
- Add 5 µL 7-AAD to every sample
- Flow cytometry analysis
    - Settings:
        - Events to record: 100 000 (live cells gate)
        - Time to record: 600s

- Volume 180 µl
- Acquiring speed: fast (60 µl/min)

Marker	Laser	Fluorescent channel	Name channel cytoflex	Fluorochrome
7-AAD	488	690/50 BP	B690-PC5.5	Percp-Cy5.5
CD56	561	585/42 BP	Y585-PE	PE
CD107	638	660/10 BP	R660-APC	eFluor660
DAAM-P	488	525/40 BP	B525-FITC	FITC

Protocol 5 – NK cell/DAAM-P complex formation assay

Reagents

- KHYG-1 cells
- Antibody coupled DAAM-P
- DAAM-P without antibody
- FACS buffer (10 mg/ml BSA, 0,5mM EDTA in PBS pH 7,4)

Set up:

Sample	Anti-LFA-1	Anti-LFA-1	Anti-LFA-1	Anti-LFA-1	Anti-LFA-1	Negative control
Concentration	25 µg/ml	8 µg/ml	2,5 µg/ml	0,8 µg/ml	0,25 µg/ml	100 µl DAAM-P protein A

Steps

1. Prepare FACS tubes with strainer cap, label, add 1 ml or 300 µl of FACS buffer, keep on ice.
2. Collect cells from culture.
3. Count cells and resuspend in medium at 10^6 cells/ml
4. Add 0,5ml (500 000 cells) to a 14 ml round-bottom tube.
5. Resuspend DAAM-P in medium.
6. Add 100 µl of DAAM-P in medium
7. Incubate in the shaking incubator at 37C, 222 RPM.
8. Measure at 15 min by transferring 100 µl through a 70 µm strainer cap to a FACS tube with 300 µl cold FACS buffer.
9. Measure at 30 min by transferring 100 µl through a 70 µm strainer cap to a FACS tube with 300 µl cold FACS buffer.
10. Measure at 1h by transferring the rest 500 µl through a 70 µm strainer cap to a FACS tube with 1 ml cold FACS buffer.
11. Directly measure FACS tubes on the flow cytometer

488	525/40 BP	B525-FITC	FITC, AF488, CFSE, Fluo-3

12. Clean & shut down FACS machine

Protocol 6 – Imaging of immune complexes in agarose

Reagents:

- 8% PFA in PBS pH 7,4 (500 µl 16% formaldehyde + 100 µl 10xPBS pH 7,4 + 400 µl H20 for 1 ml PFA)
- 1xPBS pH 7,4
- Triton X-100 stock 10%, working solution 0,2%
- Working solution Phalloidin stain 0,15 µM (400x). Stock: 66 µM (2000 units/ml)

1. Functionalize DAAM-P the day before (1,2ml of TMR DAAM-P 5kPa).
2. Collect cells from culture, spin for 5 min at 500g and resuspend in fresh medium.
3. Count cells.
4. Resuspend the cells at 10^6 cells/ml.
5. Add 0,5ml (500 000) cells to a 14 mL round-bottom tube (12 tubes in total).
6. Resuspend DAAM-P in 1,2ml medium.
7. Add 100ul DAAM-P (~10^6 per sample) at different time points (all incubations should end at the same time).
8. Incubate in the shaking incubator at 37C for 15 min, 30 min and 1h.
9. Collect samples and place on ice.
10. Add the 0,5ml sample to Eppendorf tube.
11. Add 500 µl 8% PFA in PBS pH 7,4.
12. Incubate for 10 minutes.

FOR STAINING IN AGAROSE

- Resuspend in 100 µl 1x PBS pH 7,4 with 5mM sodium azide (3 µl per ml)
- Prepare 1% and 0,5% agarose in water solution, microwave to dissolve
- Mix the cells with agarose:
    - 100 µl cells with 100 µl 1% agarose
    - 100 µl cells with 900 µl 0,5% agarose
- Transfer to wells, leave to solidify at RT
- Add 1ml 0,2% Triton in PBS
- Incubate for 1h.
- Wash with 1x PBS pH 7,4
- Add 1ml 0.15µM phalloidin in PBS solution (2,25 µl Phalloidin 400x solution per 1ml)
- Incubate overnight.
- Wash with 1xPBS pH 7,4

FOR STAINING IN TUBE

- Wash with 500 µl 1x PBS pH 7.4 + 30 mg/ml BSA , spin at 500g for 5 min.
- Add 200uL 0.2% Triton in PBS + 30mg/ml BSA.
- Incubate for 10 minutes.
- Wash with 500 µl 1x PBS pH 7.4 + 30mg/ml BSA, spin at 500g for 5 min.
- Add 200 µl 0.15µM phalloidin in PBS +30 mg/ml BSA solution (0,45 µl Phalloidin 400x solution per 200ul).
- Incubate for 30 minutes while shaking in the dark
- Wash with 500 µl 1x PBS pH 7.4 + 30 mg/ml BSA, spin at 500g for 3 min
- Resuspend in 100 µl PBS + 30 mg/ml BSA.
- Make 1% and 0,5% agarose in water solution
- Mix sample with agarose:
    - 100 µl cells with 100 µl 1% agarose
    - 100 µl cells with 900 µl 0,5% agarose
- Add to an empty well and cool at RT.

Plate setup:

	1	2	3	4	5	6
A	15 min stained in tube 2x	15 min stained in tube 10x	15 min stained in agarose 2x	15 min stained in agarose 10x		
B	30 min stained in tube 2x	30 min stained in tube 10x	30 min stained in agarose 2x	30 min stained in agarose 10x		
C	1h stained in tube 2x	1h stained in tube 10x	1h stained in agarose 2x	1h stained in agarose 10x		
D						